Electrochemical Impedance Spectroscopy Using High Order Statistics Deconvolution and Adaptive Filtering Algorithms

BY

SAEED OMAR ALJABRI

A Thesis Presented to the

DEANSHIP OF GRADUATE STUDIES

KING FAHD UNIVERSITY OF PETROLEUM & MINERALS

DHAHRAN, SAUDI ARABIA

In Partial Fulfillment of the
Requirements for the Degree of

MASTER OF SCIENCE

In

ELECTRICAL ENGINEERING

JANUARY 2012

King Fahd University of Petroleum & Minerals
DHAHRAN OF GRADUATE STUDIES

DEANSHIP OF GRADUATE STUDIES

The thesis, written by **SAEED OMAR ALJABRI** under the direction of his thesis advisor and approved by his thesis committee, has been presented to and accepted by the Dean of Graduate Studies, in partial fulfillment of the requirement for the degree of **MASTER OF SCIENCE IN ELECTRICAL ENGINEERING.**

Thesis Committee

Dr. Ahmed Yamani
Advisor

Dr. Tareq Al-Naffouri
Member

Dr. Ali A. Al-Shaikhi
Department Chairman

Dr. S. U Rahman
Member

Dr. Salam A. Zummo
Dean of Graduate Studies

18/2/12
Date

DEDICATION

This thesis is dedicated to my mother who has supported me all the way since the beginning of my studies. Also, this thesis is dedicated to my brothers, wife and children who have been a great source of motivation and inspiration.

ACKNOWLEDGMENTS

All praise and thanks are due to Almighty Allah for his guidance and continuous support for me to complete the present thesis. I bow my head with all submission and humility by way of gratitude due to Almighty Allah.

Acknowledgment is due to the king Fahd University of Petroleum and Minerals for supporting this research.

I wish to express my deep appreciation to my thesis committee chairman Dr. Ahmed Yamani for his support, guidance and valuable advice. Thanks are also extended to my thesis committee member Dr. Tarq Al-Naffouri for assisting and motivating me during my research.

In addition, I would like to express my appreciation to my thesis committee member Dr. S.U. Rahman, for assisting me in completing the experimental part of my thesis.

I would like to thank Electrical Engineering department's staff and students for their support and suggestion.

Finally, I would like to express my sincere thanks to all my family, relatives and friends for their inspiration, encouragement, and support.

TABLE OF CONTENTS

LIST OF FIGURES

LIST OF TABLES

Abstract

Name: Saeed Omar Aljabri.

Title: Electrochemical Impedance Spectroscopy Using High Order Statistics Deconvolution and Adaptive Filtering Algorithms.

Major Field: Electrical Engineering.

Date of Degree: January 2012

Electrochemical impedance spectroscopy (EIS) is one type of nondestructive testing (NDT) methods where the material's impedance is analyzed over wide range of frequencies and based on the impedance parameters, the material quality in terms of corrosion rate is determined. In this thesis, two different approaches for estimating the electrochemical impedance spectroscopies (EIS) are presented which are High Order Statistic (HOS) based deconvolution and Adaptive Filtering (AF). These two methods are proposed to overcome the drawbacks of the existing EIS techniques in terms of noise sensitivity in the case of time domain methods and the slow process speed in the case of frequency domain methods. The HOS based method treats the impedance spectrum as the unknown system frequency response in a convolution problem. Given the input signal (applied signal) and the response signal (output signal), the impedance spectrum could be estimated by the HOS based deconvolution using the third order moments of both the input and output signals. For the AF based method, the impedance spectrum is measured by estimating the parameters of the equivalent circuit representing the impedance system. Each proposed approach is analyzed with different material models and different noise statistics that usually corrupt the measurement data. MATLAB simulations and experimental results are used in the performance assessment of the two proposed methods as well as comparisons with existing methods. In comparison with the existing methods, it is shown that the proposed algorithms perform very efficiently even with the present of Gaussian and non-Gaussian distributed noises at low signal to noise ratio (SNR).

Master of Science

King Fahd University of Petroleum and Minerals

Dhahran, Saudi Arabia

ملخص الرسالة

الاسم : سعيد عمر الجابري.
العنوان: استخراج التحليل الطيفي للمقاومة الكهروكيميائية باستخدام إحصائيات عالية الرتبة و المصافي التكيفية.
التخصص : الهندسة الكهربائية.
تاريخ الرسالة: صفر 1433 (يناير 2012).

استخراج التحليل الطيفي للمقاومة الكهروكيميائية هواحد انواع أساليب الفحص اللاتلافي حيث يتم تحليل مقاومة المواد على مدى نطاق واسع من الترددات، واستنادا إلى معاييرالمقاومة، يتم تحديد نوعية المواد من حيث معدل التآكل .في هذه الأطروحة، يتم عرض نهجين مختلفين لتقدير التحليل الطيفي للمقاومة الكهروكيميائية :

I. استخراج التحليل الطيفي للمقاومة الكهروكيميائية باستخدام إحصائيات عالية الرتبة.
II. استخراج التحليل الطيفي للمقاومة الكهروكيميائية باستخدام المصافي التكيفية.

تقترح هذه الطريقتين للتغلب على العوائق المتلازمة للتقنيات الموجودة حيث حساسية الضوضاء في حالة استخدام أساليب نطاق الوقت وبطىء العملية في حالة استخدام أساليب نطاق التردد. اسلوب الاحصائيات عالية الرتبة يعامل طيف المقاومة باعتبارها استجابة نظام التردد الغير معروف في مشكلة الإلتواء .باستخدام إشارة المدخلات و الاستجابة يتم تقدير التحليل الطيفي للمقاومة الكهروكيميائية باستخدام احصائيات الرتبة الثالثة لهذه الاشارات. بالنسبة للمصافي التكيفية،يتم قياس طيف المقاومة بتقدير عوامل الدائرة الكهربائية المكافئة للنظام الكهروكيميائية.في هذه الرسالة، سيتم تحليل النهجين المقترحين مع نماذج مختلفة من المواد والإحصاءات الضوضئية المختلفة التي توجد عادة في القياس وباستخدام بيانات اصطناعية والنتائج التجريبية المقترحة فضلا عن مقارنات مع الأساليب القائمة. بالمقارنة مع الطرق القائمة ، تبين أن الطرق المقترحة تتميز بكفاءة عالية في حالة الضجيج ذو التوزيع الطبيعي و الغير طبيعي الذي قد يتداخل مع اشارات المدخلات و الاستجابة في حلة نسبة اشارة الى ضجيج ضعيفة.

درجة الماجستير في العلوم
جامعة الملك فهد للبترول والمعادن
الظهران، المملكة العربية السعودية

CHAPTER 1

INTRODUCTION

In all types of industries, the field of failure detection is very important factor that will insure the safe and quality aspects of the field operation. In the Oil and Gas industries, the corrosion is considered as the most dangerous failure that could affect a wide range of industrial components. Usually, a nondestructive testing technique (NDT) is used to insure the quality of the material and the corrosion rate without breaking down the material.

Electrochemical impedance spectroscopy (EIS) is one type of NDT method where the material's impedance is analyzed over wide range of frequencies and based on the impedance parameters, the material quality in terms of corrosion rate is determined.

The impedance's estimation is done over wide range of frequencies and this is the reason for naming this method as spectroscopy.

EIS has been introduced in the electrochemistry science since around one century and its history is thoroughly explained in references [1-5]. The research done by Oliver Heaviside in the time frame of 1880-1900 was the foundation of the EIS technology [2]. Oliver Heaviside created a useful transformation that solves differential equations in terms of simple (simultaneous) algebraic equations in the Laplace domain. These transformations which are (s=d/dt) and (1/s=$\int$dt) are considered as the foundation of the operational calculus. The Heaviside transformation defines the term "impedance" in terms of voltage and currant as follows:

$$Z(s) = \frac{V(s)}{I(s)} \tag{1-1}$$

where V(s) and I(s) are the Laplace transform of the voltage and current signals respectively. It is worth to mention that the previous impedance relation is valid in the case of steady state linear system (LS). In order to have a linear impedance system, the following four conditions should be satisfied [2]:

1. The system response is written by linear differential equations and hence the superposition principle is applicable.

2. The system is stable.
3. The system is causal.
4. The impedance should be finite.

The second revolution in the EIS techniques was done by Warburg in 1899 where he wrote a remarkable paper on the analysis of diffusion impedance for an electrocative species. In 1950, the main EIS's application was the determination of interfacial impedance using reactive bridge techniques such as Wheatstone and Berberian-Cole bridges [2, 4]. The main disadvantage of the bridge technique is the low frequency limitation such that the minimum measurable frequency is 100 Hz. Despite its limitation, the reactive bridge based EIS was utilized heavily in the measurement of double layer capacitance at solid and liquid metal electrodes. At that time, the EIS was not used in the analysis of corrosion and electro dissolution reaction until the work done by Epelboin and his group in 1960 in Paris. The Epelboin's group along with SOLARTRON instruments, Ltd developed the instrument called frequency response analyzer (FRA). The FRA is a device which determines the frequency response of a measured system and the FRA called SOLARTRON 1172 is considered as the leader in this filed [3]. The FRA has a minimum measured frequency of 0.1m Hz which enables the analysis of corrosion reaction, coupling between charge transfer, chemical, and mass transfer process. The FRA is applicable for measuring

frequency response of linear systems that satisfythe previous four conditions. For the past fifteen years, a method called Kramers-Kronig (K-K) transformation is used to check the compelling of the impedance data with the constraints of the linear system theory [6]. The K-K transforms were initially developed in 1920 to examine optical data. The K-K transforms depends on the Cauchy's theorem which relates the realand imaginary parts of the impedance data to each other as per the following equations:

$$Z_{real}(w) = Z_{real}(\infty) + \frac{2}{\pi}\int_0^{\infty} \frac{XZ_{imag}(x) - wZ_{imag}(w)}{x^2 - w^2} dx$$

or

$$Z_{real}(w) = Z_{real}(0) + \frac{2w}{\pi}\int_0^{\infty} \frac{(w/x)Z_{imag}(x) - Z_{imag}(w)}{x^2 - w^2} dx \qquad (1\text{-}2)$$

$$Z_{imag}(w) = -\frac{2w}{\pi}\int_0^{\infty} \frac{Z_{real}(x) - Z_{real}(w)}{x^2 - w^2} dx$$

where $Z_{real}(w)$ and $Z_{imag}(w)$ are the real and imaginary parts of the impedance spectrum Z (w) respectively. In order to have a valid impedance data, the K-K transform equations should be satisfied.However, the utilization of the K-K transforms is limited by two drawbacks, which are: limited frequency range and the presence of the noise [6].

The FRA based EIS measurement had two main weaknesses such that it requires long data acquisition time and it is costly ($20,000 for the basic FRA) [4].

To overcome the FRA's drawbacks and the demand for real time EIS applications, a Fast Fourier Transform (FFT)-based EIS was developed recently. In this technique, a perturbation signal (voltage or current) is applied across the electrochemical system and the impedance is measured in terms of the Fourier transform of voltage and current signals. Although the FFT-based method gives a fast impedance spectroscopy measurement, it is affected by noise since the response for all frequencies are measured at the same time. This applies for dynamic range system as corrosion coating model where magnitude of the system response is varying dramatically across the frequency spectrum. This is clearat the high frequency side of the spectrum where the measured current is high because of low impedance and vice versa at the low frequency end of the spectrum. As a result, noisy measurement data is obtained at the low frequency side and clipped data at the high frequency side [4].

1.1 Thesis Objective

The EIS's history shows that there are two main categories of EIS techniques: frequency domain methods and time domain methods. The FRA is one example of the frequency domain methods which gives reliable impedance measurements at the expense of long acquisition time, cost and complexity. Therefore, the FRA is not applicable for real time applications. On the other hand, the FFT based method which belongs to the time domain techniques is much faster than the FRA but with less reliability and accuracy because of the dynamic range deficiency. So, the main objective of this thesis is to propose simple and fast EIS techniques that will produce reliable impedance data in noisy environment.

In this thesis, two different approaches for estimating the electrochemical impedance spectroscopy are presented which are High Order Statistic deconvolution based methods (HOS) and Adaptive Filtering based method (AF). For each technique, the estimation performance is analyzed for different electrochemical models with additive Gaussian and non-Gaussian noise signals.

The overall objectives of this thesis are:

1. Applying High Order Statistic (HOS) based Deconvolution technique for determining the impedance spectrum of a coated metal pipe.
2. Using different adaptive filtering (AF) algorithms in determining directly the parameters of the equivalent circuit representing the electrochemical systemof acoated metal pipe.
3. Analyzing the performance of both proposed approaches in the case of additive Gaussian and non-Gaussian noise. The performance assessment is measured in terms of normalized estimation error versus different signal to noise ratio (SNR).
4. Determining the factors that could affect the accuracy of the two methods.
5. Comparing the performance of the two proposed methods with existing EIS techniques based on MATLAB simulation and experimental result.

1.2 Thesis Organization

This thesis consists of 8 chapters. Chapter 2 gives an overall review and analysis of the existing electrochemical impedance spectroscopy methods. The background and basics of high order statistics deconvolution based method are described in chapter 3.In chapter 4, simulation results using MATLAB software are illustrated to demonstrate the performance index of the HOS-based EIS method. The second

proposed EIS measurements technique which is AF is explained thoroughly in chapter 5. The AF-based EIS performance using simulation results are summarized in chapter 6 while chapter 7 compares the performance of the two proposed method with spectroscopy instrument called VMP3. Finally, summary of the main results and conclusion are given in chapter 8.

CHAPTER 2

Review of Existing Electrochemical Impedance Spectroscopy (EIS) Techniques

The EIS technology development is a continuous and challenging task where several scientific researches are conducted in this filed on yearly bases. The main objective of these researches is to enhance the capabilities and reliability of the EIS technique.

The EIS has wide range of applications such as material evaluation, corrosion protection, evaluation of properties, quality control and capacity estimation of batteries [7]. There are different EIS techniques, which could be classified into three main categories: Phase Sensitive Detection (PSD) based method, Frequency response analyzer (FRA) based method and Fast Fourier Transform (FFT) based methods.

2.1 Phase Sensitive Detection based method

The phase sensitive detection is utilized in the lock-in amplifier which has the capability to extract a signal from noisy measurement. In PSD, the impedance spectrum is estimated by measuring the frequency response at each frequency in

terms of amplitude and phase (polar form). An AC voltage is applied across the impedance system at particular frequency and the amplitude and phase of the response current signal are calculated. The output current signal is usually distorted by additive noise signal that could be filtered out using the PSD algorithm. In PSD, the output signal will pass through two consecutive stages. In the first stage, the output signalis multiplied bya reference signal and the output of the multiplication processis:

$$E_1E_{\ 2}=\frac{2E_1}{\pi}\left\{\begin{array}{l}\cos(\varphi_1-\varphi_2)-\cos(2wt+\varphi_1+\varphi_2)\\+\frac{1}{3}\cos(-2wt+\varphi_1-3\varphi_2)-\frac{1}{3}\cos(4wt+\varphi_1+3\varphi_2)\\+\frac{1}{5}\cos(-4wt+\varphi_1-5\varphi_2)-\frac{1}{5}\cos(6wt+\varphi_1+5\varphi_2)+....\end{array}\right\} \quad (2\text{-}1)$$

While $(E1,\varphi_1)$ and $(E2,\varphi_2)$ are the amplitudes/phase of the output currentand the reference signals respectively, w is the angular frequency. The main objective of the second stage is to eliminate the time dependent components of the above signal and this can be achieved by passing the multiplication output signal through a low pass filter that produces the following signal:

$$\frac{2E_1}{\pi}\cos(\varphi_1-\varphi_2) \quad (2\text{-}2)$$

The amplitude of the filter's output signal is proportional to the amplitude of the output current signal (E_1) and it reaches its maximum value when the phase difference between the current and the reference signals is zero. The phase part of the frequency response is obtained in similar way as the amplitude component. The only modification is related to the reference signal, which needs to be shifted by (π/2). Since the PSD measures the frequency response at a particular frequency, the two PSD's steps are repeated for all frequencies in order to produce the complete impedance spectrum. The operational frequency range of the PSD is between 0.5-100000 Hz with a precision of 0.1 to 0.2% [8].

The main advantages of PSD are noise removal, sensitivity, harmonic distortion reduction and low cost. On the other hand, the PSD has limited operational frequency and consumes a lot of time and these two criteria's are considered as the main disadvantages. A schematic operation diagram of PSD is shown below:

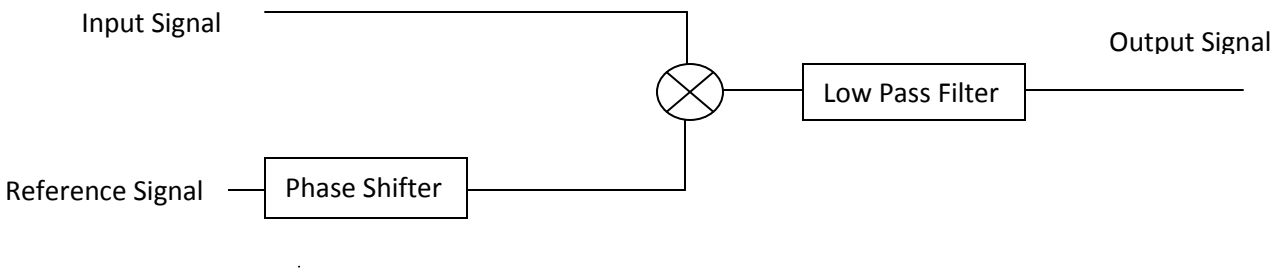

Figure 2.1 A schematic operation diagram of PSD

2.2 Frequency Response Analyzer based method

The FRA shares with the PSD the same principle of measuring the impedance spectrum which is applying a sinusoidal signal at a particular frequency. However, the FRA estimates the impedance spectrum in terms of the real and imaginary parts of the frequency response (rectangular form). In FRA, the output signal is multiplied by sine and cosine signals whose frequency is same as the input signal. After that, the real and imaginary parts of the response signal are obtained by integrating the multiplication's output signal over one or more periods:

$$\mathrm{Re}(E1) = \frac{1}{T}\int_0^T E1\sin(wt+\varphi_1)\sin(wt)dt = \frac{E1}{2}\cos(\varphi_1)$$
$$\mathrm{Im}(E1) = \frac{1}{T}\int_0^T E1\sin(wt+\varphi_1)\cos(wt)dt = \frac{E1}{2}\sin(\varphi_1) \quad (2\text{-}3)$$

This process is repeated for all frequencies in order to measure the impedance's frequency response. FRAcan reject all harmonic signals that could affect the accuracy of EIS measurements [8].The FRA based methods has several advantages such as fast analysis compared with PSD based method, wide frequency range, harmonic distortion removal, direct output to external device and easy standalone measurements [8].The main disadvantages of FRA are the need of a complex signal generator/phase sensitive devices, limited noise removal compared with the PSD based method, limited sensitivity and long measurement time to get the impedance of wide frequency range [8, 9]. Also, the reference signal is applied at least for two periods in order to eliminate the transient effect.

2.3 Fast Fourier Transform (FFT) based method

The recent scientific papers and researches conducted in the EIS field are mainly in the area of Fast Fourier Transform based EIS method [10, 11]. This is because the ability of this technique to measure the impedance in real time basis. FFT-based algorithm is used in many applications when the measurement's speed is essential factor such as estimation of battery impedance, analysis of transient electrochemical processes and studying the characteristics of biological materials [12, 13]. The FFT

technique depends on the fact that the system impedance is the ratio of the Laplace transform of voltage and current signals:

$$Z(s) = \frac{E(s)}{I(s)} \tag{2-4}$$

For the purpose of estimating the impedance spectrum, a perturbation signal is applied to the system and the impedance spectrum is measured by getting the ratio of the Fourier transform of both the input and output signals. The Fast Fourier transform is a quick and an efficient method for calculating the Fourier transform of a signal and it is used here to reduce further the time required of the EIS process.There are several requirements that need to be satisfied in selecting the applied signal. First, the magnitude of the applied signal should be small such that the response of the system remains linear [7]. Second, the applied signal's frequency spectrum needs to be wide as possible. Also, there should be no coincidence of harmonics frequencies in order to minimize the non-linear faradic current interference [14]. The fourth requirement is related to the sampling rate of the signal which should be calculated as per the Nyquist theorem. While the sampling rate determines the maximum measurable frequency of the electrochemical system, the lowest measured frequency (frequency resolution) is specified by the reciprocal of the total sampling time [14].The applied

signal could be any arbitrary signal having wide range of frequency and in practice the input signal is either:a pulse,a noise or sum of sine waves [14, 15].

For noise perturbation, white noise is usually utilized as applied signal since it has a continuous frequency spectrum. However, the immunity of the noise is weak because the amplitude of single frequency component of the white noise obtained by the FFT is relatively low [8].

The sum of sine waves signal consists of a fundamental harmonic frequency f_o and number of odd harmonics frequencies ($(2n+1)f_o$) [15].A proper selection of both the amplitude and phases of the individual sine wave are made to reduce the peak-to-peak amplitude of the signal. At the same time, the amplitude of the individual frequency components is increased. Accordingly, the linear nature of the studied system is maintained as well as the noise immunity of the impedance measurement is improved. The drawback of this applied signal is the need of a sophisticated hardware and it does not measure the impedance spectrum over the whole range of the low frequency band. This is because the applied signal should have the property of non-overlapping of the second harmonics [9,16].

Alternative choice of the applied signal is a pulse with wideband frequency such as Dirac's delta function (δ (t)). However, such a function cannot be generated

practically and it is replaced by a pulse of short duration, which has weak frequency response at high frequencies. This will make a low-level noise signal affects the impedance measurement significantly [8]. To utilize the advantages of the delta function and overcome the difficulties in generating such signal in practical, the delta function could be substituted by its integrated form. After that, the equivalent delta pulse's response is obtained by taking the derivate of the system response [16, 17, 18].

In general, the main advantage of the FFT based method is that the impedance spectrum is measured quickly compared with the FRA based method andhence it is utilized in the real time EIS applications. In addition, there is no need for the phase sensitive detector that will simplify the required hardware [9]. However, the FFT based method has several disadvantages like the PSD and FRA based methods. First, it has limited converge at the low frequency side of the impedance spectrum. Moreover and unlike the FRA based method, the output signal is usually noisy and weak [8].The reference "Fully Integrated Impedance Spectroscopy Systems for Biochemical Sensors Array" [19] compares the performance of the FRA and FFT based methods.

It is clear that there is a contradiction between the time required of the impedance measurement and the immunity of noise. It is noticed also that both the FRA and FFT methods do not consider the removal of the noise during the impedance measurement. It is obvious that the noise could lead to wrong impedance spectrum estimation and as a result the EIS will not meet the planned objectives [20]. This raises the need of alternative algorithms, which will accomplish both the removal of the noise and measuring the system impedance in a reasonable time.

CHAPTER 3

REVIEW OF HIGH ORDER STATISTICS BASED DECONVOLUTION

There are different types of deconvolution algorithms such as wiener filtering, least square error and High Order Statistics based deconvolution. The first two types depend on the first and second order statistics (SOS), which are the mean and variance. Both wiener filtering and least square error can only estimate the system impulse response for high signal to noise ratio (SNR). The precision of the deconvolution estimation depends on the nature of the system (minimum phase system or non-minimum phase system) and noise statistics (Gaussian/uniform/Rayleigh). Alinear time invariant system is considered to be minimum-phaseif the system and its inverse are causal and stable. Whilea non-minimum phase system is stable, its inverse is not stable. The SOS deconvolution does not estimate the impulse response properly for non-minimum phase systems,

which is the nature of the majority of the electrochemical system representing a coated metal.

In addition, the SOS deconvolution performance in terms of noise removal is optimum for the additive Gaussian noise corrupting the output signalonly. [21]

On the other hand, advanced deconvolution approaches (HOS) show significant improvement in terms of deconvolution accuracy in the case of non-minimum phase systems and non-Gaussian distributed noise signal that distorts both the input and output data. Therefore, this thesis investigates the possibility of utilizing the HOS deconvolution in the EIS application measurements.

3.1 High order Statistic (HOS) Deconvolution

The HOS technique is utilized in many applications such as identification of finite impulse response (FIR) system, detection of non-Gaussian noise, identification of linear time invariant system (LTI) and stochastic realization... etc. [22]. This technique has the ability to keep the phase information, which is helpful in NDT applications [21].

The HOS deconvolution depends on high order moment (cumulant), which equals zero for Gaussian signals, and hence the HOS can distinguish the nature of the process.

The cumulant determines how close the distribution of a random process from being Gaussian distributed signal and it is calculated as follows [22]:

$$c_k^n(k_1,k_2,..k_{n-1}) = m_n^x(k_1,k_2,..k_{n-1}) - m_n^G(k_1,k_2,..k_{n-1}). \quad (3\text{-}1)$$

Where m_n^x (x) is defined as the nth order moment for a stationary random process and it is defined as:

$$m_n^x(k_1,k_2,...k_{n-1}) = E\{x(k)x(k+k_1)...x(k+k_{n-1})\}. \quad (3\text{-}2)$$

whereE { } is the statistical expectation operator.

$m_n^G(..)$ is the nth order moment for a Gaussian random process that has the same second order statistics of the signal (x).Note that, for a Gaussian random process, the high order cumulants are identically zero.

For a random process whose mean equals zero, the first, second, third and fourth cumulants could be simplified to the following:

$$\begin{cases} c_1^x = m_1^x = 0 \\ c_2^x(k_1) = m_2^x(k_1) \\ c_3^x(k_1,k_2) = m_3^x(k_1,k_2) \\ c_4^x(k_1,k_2,k_3) = m_4^x(k_1,k_2,k_3) - m_2^x(k_1)m_2^x(k_3-k_2) - m_2^x(k_2)m_2^x(k_3-k_1) - m_2^x(k_3)m_2^x(k_2-k_1) \end{cases}$$

In HOS deconvolution, other measurements are used which are nth order spectrum and nth order cepstrum. The nth order spectrum is the Fourier transform of the correlation function of a stationary ransom process.

The 2nd order spectrum (bi-spectrum) is:

$$C_3^x(w_1,w_2) = F_2[c_3^x(k_1,k_2)] \text{ .(3-3)}$$

While the 3rd order spectrum (tri-spectrum) is:

$$C_4^x(w_1,w_2,w_3) = F_3[c_4^x(k_1,k_2,k_3)] \text{ .} \quad \text{(3-4)}$$

The nth order cepstrum is the inverse Fourier transforms of the above equations. There are two HOS techniques for identifying the impulse response, which are the parametric and the non-parametric approaches. For the parametric technique, the first step is to find the parameters of nominator and denominator representing the Z-transform of the system frequency response [23]. After that, the impulse response is obtained by taking the inverse Fourier transform of the estimated frequency response.The non-parametric methoduses the cumulants, bi-cepstrum and tri-

cepstrum to determine directly the impulse response of the system. In this thesis, a specific type of parametric HOS deconvolution is employed which depends on 3rd order cumulant.

3.2 HOS Deconvolution using 3rd order cumulants

This technique is fully explained in references [24-28]. InHOS based Deconvolution, the tested system is usually assumed to be a linear time invariant, causal and stable with absolutely summable impulse response. In addition, the input signal should be non-Gaussian, zero-mean and i.i.d signal with non-zero high order moments. Moreover, the input's noise and output's noise are considered to be zero-mean, mutually correlated Gaussian random process and independent of the input signal. The last assumption is that the estimated model order satisfies the following inequalities:

$$n_a \geq m, n_b \geq n \tag{3-5}$$

while n_a and n_b are the estimated system order of the dominator and nominator respectively, m and n are the true system order.

In HOS based Deconvolution, the system model is [29]:

$$w(t) = -\sum_{i=1}^{n_a} A_i w(t-i) + \sum_{i=1}^{n_b} B_i v(t-i) \tag{3-6}$$

where w (t) and v (t) are the output and input signals respectively and A_i and B_i are the unknown parameters of the system frequency response:

$$H(Z) = \frac{B_3 z^3 + B_2 z^2 + B_1 z + \ldots B_{n_b}}{A_3 z^3 + A_2 z^2 + A_1 z + \ldots A_{n_a}} \tag{3-7}$$

Usually, both the input and output are distorted by noise signals resulting to the following modified input and output signals:

$$\begin{aligned} y(t) &= w(t) + n_y(t) \\ x(t) &= v(t) + n_x(t) \end{aligned} . \tag{3-8}$$

Where the $n_y(t)$ and $n_x(t)$ are the output and input noise respectively. The system block diagram is shown below [29]:

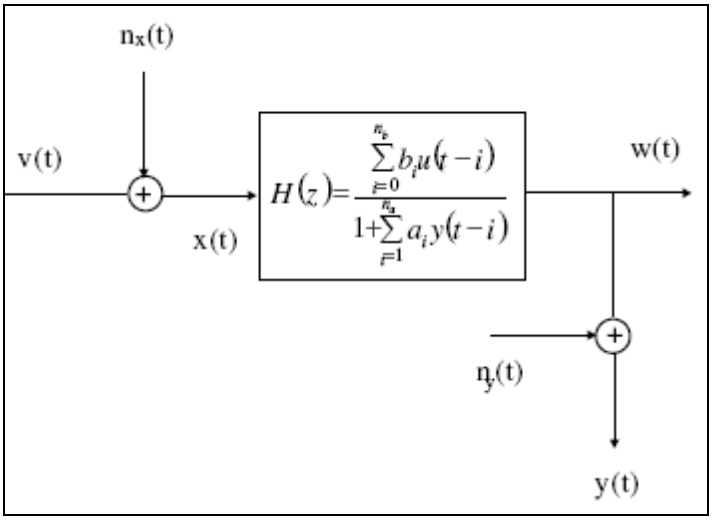

Figure 3.1 Block diagram of the system model [18]

As a result, the system model can be rewritten as:

$$y(t)+\sum_{i=1}^{n_a} A_i y(t-i)=\sum_{i=1}^{n_b} B_i x(t-i)+n(t). \tag{3-9}$$

where

$$n(t)=\sum_{i=1}^{n_a} A_i n_y(t-i)+\sum_{i=1}^{n_b} B_i n_x(t-i). \tag{3-10}$$

The third order cross-cumulants between the input and output signals is defined as follows [29]:

$$c^{vwv}(\tau_1,\tau_2)=E[v(t)w(t+\tau_1)v(t+\tau_2)] \tag{3-11}$$

This cross cumulants can be approximated from the sample average of both the input and output data as follows:

$$\hat{c}^{vwv}(\tau_1,\tau_2)=\frac{1}{N}\sum_{t=0}^{N-1}[v(t)w(t+\tau_1)v(t+\tau_2)]. \tag{3-12}$$

where N equals the number ofsamples. The 3rd order cumulants based deconvolution is based on several cumulants's properties, which are:

1. Multilinearity:

   The cumulants are linear with respect to each of their arguments:

   $$cum[\sum_i \alpha_i x(t_i),\sum_j \beta_j x(t_j),\sum_k \gamma_k x(t_k)]=\sum_{i,j,k}\alpha_i\beta_j\gamma_k cum[x(t_i),y(t_j),z(t_k)]$$

2. Additively:

   The sum of the cumulants equals the cumulants of the sum:

   $$cum[x(t_1)+y(t_1)+....+x(t_n)+y(t_n)]=cum[x(t_1)+....+x(t_n)]+cum[y(t_1)+....+y(t_n)]$$

3. The third order cumulants of a random variable which has symmetric distribution density function is zero [30].

Based on the previous properties, the impulse response of a linear system is written in terms of the auto and cross cumulants:

$$c^{vwv}(\tau_1,\tau_2)=\sum_{t=-\infty}^{\infty}h(t)c^{vvv}(\tau_1-t,\tau_2) \quad . \tag{3-13}$$

where h (t) is the system impulse response. The (3.13) can be rewritten as the following formula using compact notation:

$$c^{vwv}(\tau_1,\tau_2)=\frac{B(q^{-1})}{A(q^{-1})}c^{vvv}(\tau_1-t,\tau_2). \tag{3-14}$$

where q^{-1} is the unit delay operator. The proof of the previous relation is explained below [30]:

$$c_{vwv}(\tau_1,\tau_2)=c_{v_o w_o v_o}(\tau_1,\tau_2)$$

$$=E[v_o(t_k)w_o(t_k+\tau_1)v_o(t_k+\tau_2)]$$

$$=E\left[v_o(t_k)\left(\int h(\tau)u_o(t_k+\tau_1-\tau)d\tau\right)v_o(t_k+\tau_2)\right]$$

$$=\int h(\tau)E[v_o(t_k)v_o(t_k+\tau_1-\tau)v_o(t_k+\tau_2)]d\tau$$

$$=\int h(\tau)c_{v_o v_o v_o}(\tau_1-\tau,\tau_2)d\tau$$

$$=H(p)c_{v_o v_o v_o}(\tau_1,\tau_2)=H(p)c_{v\,v\,v}(\tau_1,\tau_2)$$

Using the noisy input and output signals (y(t),x(t)) instead of w(t) and v(t),an error signal (e) is generated:

$$e(\tau_1,\tau_2,\theta)=A(q^{-1})\hat{c}^{xyx}(\tau_1,\tau_2)-B(q^{-1})\hat{c}^{xxx}(\tau_1-t,\tau_2). \quad (3\text{-}15)$$

$$\theta=[a_1,.....a_{na},b_1,.....b_{nb}]$$

The objective of 3rd order cumulant based deconvolution is to find the system parameters, the vector θ, by minimizing the following cost function, which is in terms of the error signal (e):

$$j(\theta;\tau_2)=\frac{1}{M}\sum_{\tau_1=1}^{M}\frac{1}{2}[e(\tau_1,\tau_2,\theta)]^2 . \quad (3\text{-}16)$$

In order to find the least square solution for the above cost function, the error signal is rewritten as:

$$e(\tau_1,\tau_2,\theta)=\hat{c}^{xyx}(\tau_1,\tau_2)-\hat{\phi}^{T}(\tau_1,\tau_2)\theta \quad . \quad (3\text{-}17)$$

where,

$$\hat{\phi}(\tau_1,\tau_2)=\left[-\hat{c}^{xyx}(\tau_1,\tau_2),.....-\hat{c}^{xyx}(\tau_1-n_a,\tau_2),\hat{c}^{xxx}(\tau_1-1,\tau_2),.....\hat{c}^{xxx}(\tau_1-n_b,\tau_2)\right]^T \quad (3\text{-}18)$$

Giving the τ_2 specific value (e.g., τ_2 =0), the least square algorithm yields the following solution:

$$\hat{\theta}^{M} = \left[\frac{1}{M}\sum_{\tau_1=1}^{M}\hat{\phi}(\tau_1,\tau_2)\hat{\phi}^{T}(\tau_1,\tau_2)\right]^{-1}\left[\frac{1}{M}\sum_{\tau_1=1}^{M}\hat{\phi}(\tau_1,\tau_2)\hat{c}^{xyx}(\tau_1,\tau_2)\right]. \quad (3\text{-}19)$$

The HOS deconvolution using 3rd order cumulants correctly estimates the impulse response of digital MPS and NMPS [29]. There are many factors that affect the accuracy of the estimation such as the model assumed order ($n_{a,}n_b$). If the difference of the assumed nominator and denominator orders is the same as for the true system, the estimation of the HOS based deconvolution is perfect [29]. Another factor that affects the deconvolution precision is the parameter 'M' which is used in the definition of the cost function and it is called the cumulants maximum lag [30, 31]. The effect of these two parameters is analyzed further in the next chapter. To demonstrate the performance of the 3rd order cumulants based deconvolution-based method; consider the following two digital minimum and non-minimum phase systems:

$$H_{\min phase} = \frac{z+0.2}{z^3+0.5z^2+0.72z+0.068}$$

$$H_{\max phase} = \frac{0.2z+1}{z^3+0.5z^2+0.72z+0.068} \quad (3\text{-}20)$$

The impulse response of these two digital systems has oscillatory nature in order to test the robustness of the HOS based deconvolution [21]. The two systems are excited by the input signal:

$x(t) = e^{-\left(\frac{2\pi f_0}{\sigma} t\right)^2} \cos(2\pi f_0 t)$ that will generate an output signal, whichis sequentially distorted by a Gaussian/Non-Gaussian noises signals. The noisy output will be the input of the HOS deconvolution filter. Figure (3.2) shows both the true and estimated system impulse response for the minimum phase and non-minimum phase system with output's SNR of 20 dB.

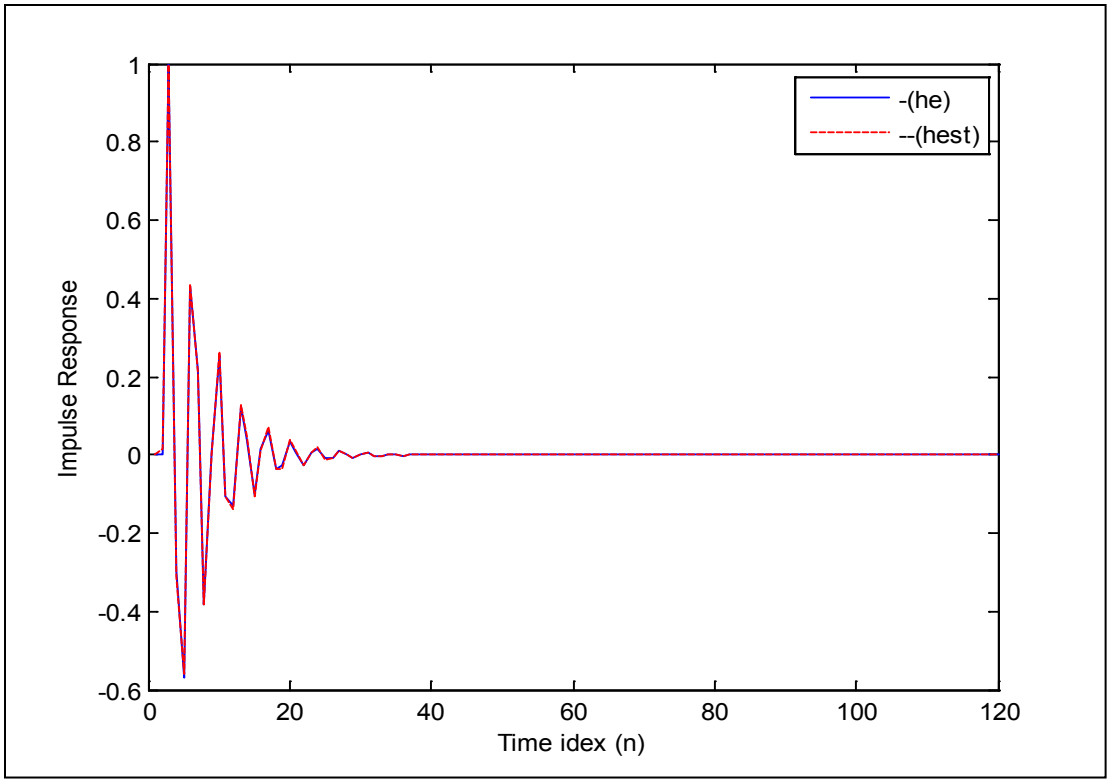

Figure 3.2a: Actual (blue line) and estimated (red line) impulse responses for output's SNR = 20 dB Gaussian noise for Minimum Phase System (MPS)

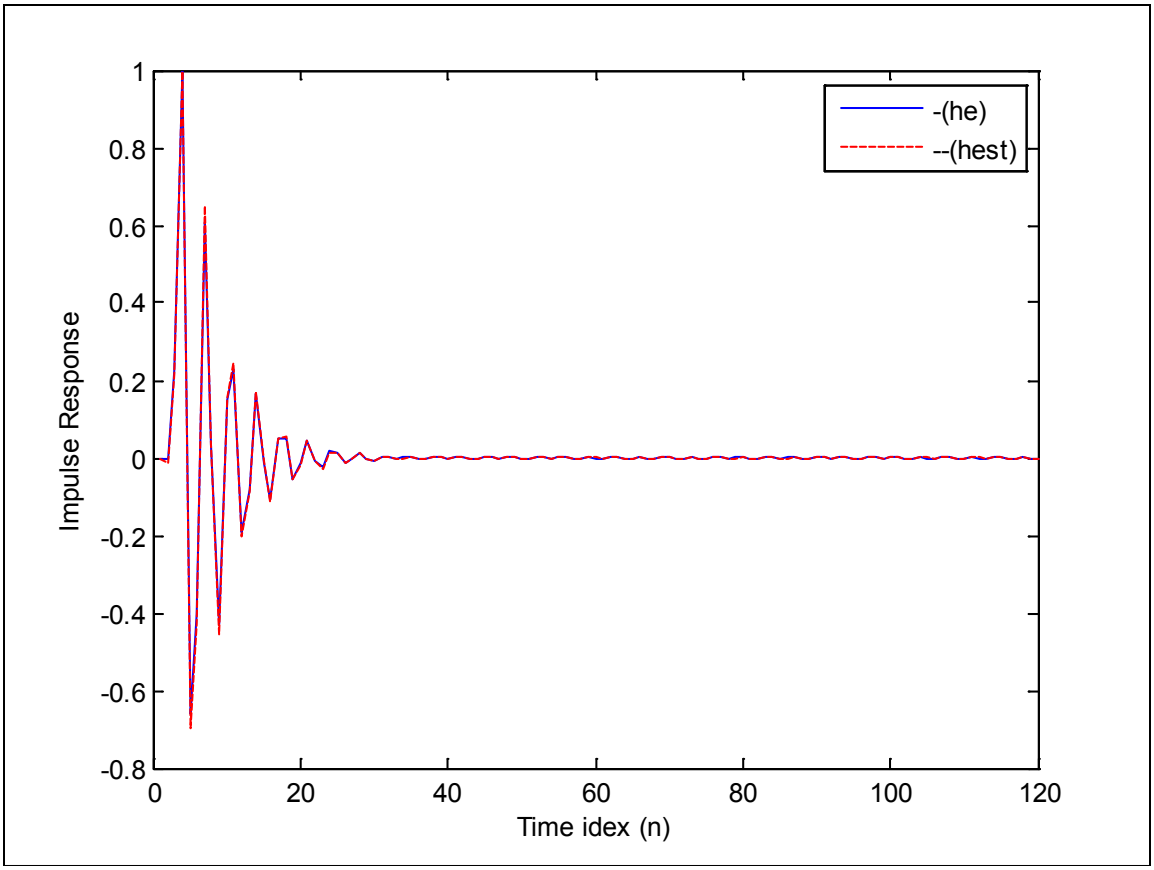

Figure 3.2b: Actual (blue line) and estimated (red line) impulse responses for output's SNR = 20 dB Gaussian noise for non-Minimum Phase System (NMPS)

Table 3.1 shows the reset of the estimation results obtained at different values of output's SNR:

System	SNR(dB)	Estimation error (%)
Minimum phase	20 (Gaussian)	5.33e-2
Minimum phase	5 (Gaussian)	0.75
Minimum phase	20 (non-Gaussian)	6.38e-2
Minimum phase	5 (non-Gaussian)	3.5
Maximum phase	20 (Gaussian)	7.87e-2
Maximum phase	5 (Gaussian)	4.12
Maximum phase	20 (non-Gaussian)	1.3
Maximum phase	5 (non-Gaussian)	5.8

Table 3.1: Impulse response's estimation error vs. output's SNR using 3rd order HOS based Deconvolution

As per the above results, the HOS based deconvolution using 3rd order cumulants precisely estimates the impulse response of digital MPS and NMPS. The HOS based deconvolution keeps the perfect performance even when the output data is contaminated with additive Gaussian or non-Gaussian noises.

3.3 EIS Measurements Using 3rd Order Cumulants HOS Deconvolution based method:

The HOS based EIS measurement is modeled as a convolution problem[29]. Here, the required impedance spectrum is assumed to be the unknown frequency response that can be estimated using a deconvolution filter. The inputs of the deconvolution filter are the arbitrary applied signal of the system as well as the output signal. The main advantage of this approach is the ability to estimate the impedance spectrum (system response) perfectly even with present of the noises unlike the FFT-based method.

In this thesis, the electrochemical system is considered as a coated metal pipe, which can be represented by several electrical circuit models. Figure 3.3 shows the most generic electrical circuit representing a coated metal pipe.

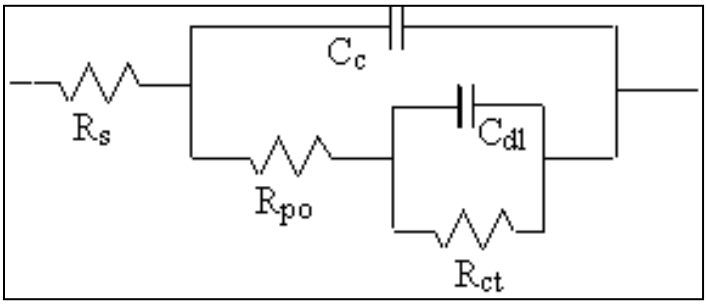

Figure 3.3: Equivalent Circuit of pipeline coating [41]

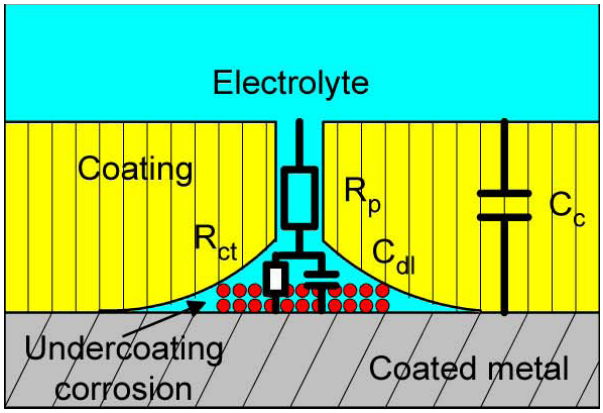

Figure 3.4:Coating modeling example. [8]

R_s represents the electrolyte resistance whereas $R_{po}$and $C_c$represent the polarization resistance and coating capacitance respectively. On the other hand, $R_{ct}$is the charge transfer resistance, which is inversely proportional to the corrosion rate. C_{dl} is the double layer capacitance at the electrode-electrolyte interface. Usually, the value of these model's parameters are changing during the life of the coating such that R_{po}, R_{ct} and C_{dl} do not exist when the coating is new [32]. While R_{ct} and C_{dl} will be seen in the picture as the corrosions starts, the C_c and R_{po}become unfeasible when the coating breaks up.

The EIS measurement of the electrochemical system (coated metal) is models as convolution problem as shown in Figure 3.5.

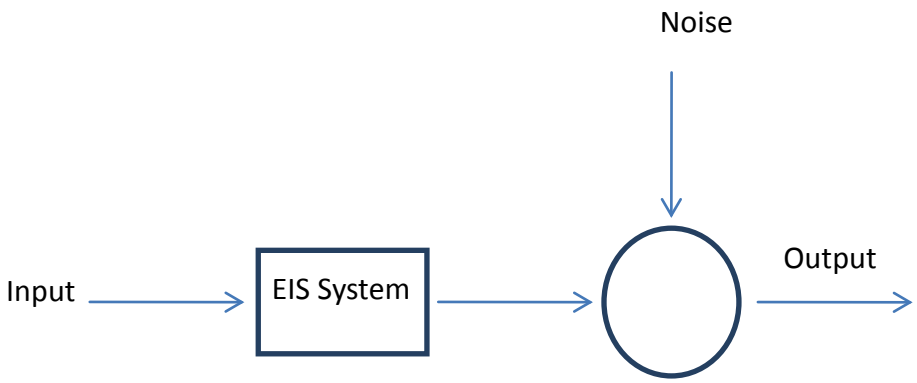

Figure 3.5: EIS Convolution model

In this convolution model, the input signal is either a current (galvonostatice mode) or a voltage (potentiostatice mode) signals.in addition, the input and output signals are distorted by noise signals generated by different probability density function (Gaussian, Uniform and Rayleigh). The mathematical expression of this model is:

$$y(t) = i(t) \otimes Z(t) + n(t) \tag{3-21}$$

Z (t) is the inverse Fourier transform of the impedance spectrum Z (w) and n (t) is the noise. Once the Z (w) is estimated, a curve fitting technique is used to estimate the electrical circuit's parameters based on complex nonlinear Least squares method

(CNLS) [33, 34]. The goal of the CNLS is to find a set of parameters P that will decrease the following cost function:

$$S(P) = \sum_{M} W_j \left[Y_j - YC_j(P) \right]^2 \tag{3.22}$$

M is the number of measurement data and W_i is the weight associated withj^{th} observation point Y_j. $YC_j(P)$is a function in terms of the parameters (P) whose curve tracks the observation's curve. This technique can handle complex data by splitting the real and imaginary part in a single array which double the data point's number from M to 2M.

The original objective of 3rd order cumulants Deconvolution is to estimate the impulse response of LTI digital system [24,25,26].On the other hand, the EIS aims to find the impedance spectrum of continuous electrochemical system rather than the impulse response. There are two approaches in order to find the impedance spectrum using the HOS based method. In the first approach, the Fast Fourier transform is utilized to convert the estimated impulse response to the required frequency response. However, this approach will not estimate the amplitude of the spectrum perfectly as the phase side. The amplitude of the estimated impedance spectrum needs to be amplified to match the true impedance.

The second approach is to find the impedance spectrum from the estimated Z-transformof the equivalent digital system directly rather than the estimated impulse response. The continuous transfer function (Laplace transform) is obtained by converting the transfer function from the Z-domain to the S-domain using the available methods such as zero-order hold, first –order hold, Tustin approximation and matched poles and zeros methods. As a result, the use of the Fast Fourier Transform (FFT) is avoided. The FFT of a digital signal is defined as follow:

$$X(K) = \sum_{n=1}^{N} x(n) \exp(\text{-j*2*}\pi\text{*(K-1)*(n-1)/N}) \tag{3-23}$$

Where, N is the length of the digital sequence. The precision and the speed of the FFT calculation depend on the length of the signal (N).As the signal is padded with zero, the accuracy of the FFT increases. In addition, the final result of the FFT needs to be normalized with the signal's length (N). So, the length N could affect the accuracy of the estimated impedance spectrum and this could be the reason of the amplitude estimation error. Fortunately, the use of the FFT would be avoided by using the second approach and hence it will be used in this thesis.

CHAPTER 4

PERFORMANCE OF EIS HOSDECONVOLUTION BASED METHOD (SIMULATION RESULT)

In this chapter, a comparison is done between the performance of the HOS-based EIS and the conventional method (FFT-based) in estimating the impedance spectrum of electrochemical system representing a coated metal. This comparison considers additive Gaussian noise distorting either the output signal only or both the input and output signals. Also the test is done for both new coating metal model and bad (corroded) coating metal model in order to measure the robustness of the proposed method during the life cycle of the coating. The parameters of the circuit model representing the new and corroded coating are listed in the Table below [32].

Parameter	New Coating	corroded coating
R1(Rpo)Ω	100e6	1e6
R2(Rct)Ω	500e6	5e6
C1(Cc)F	100e-12	400e-12
C2(Cdl)F	10e-12	10e-9

Table 4.1: Circuit parameters representing new and bad coating metal pipe

The electrolyte resistance (Rs) is neglected in the test.A MATLAB program simulates the test and the Toolbox named "High order Spectral-Analysis'' is utilized for the pre-defined functions used in the program [31]. The simulation tests consists of four different cases:

1. The new coating model with noisy output (Gaussian noise).
2. The new coating model with noisy input/output (Gaussian noise).
3. The corroded coating model with noisy output (Gaussian noise).
4. The corroded coating model with noisy input/output (Gaussian noise).

4.1 Case#1(The new coating model with noisy output (Gaussian noise)

In this test, the performance of the two methods is measured in terms of the normalized estimation error:

$$\left\| \frac{|H(f)| - |\hat{H}(f)|}{|H(f)|} \right\| \times 100 \qquad (4\text{-}1)$$

$H(f)$ and $\hat{H}(f)$ are the true and estimated impedance spectrums respectively. The normalized estimation error is calculated at different output's SNR. The result of the comparison is summarized in Table 4.2 and Figure 4.1:

SNR(dB)	Normalized Estimation Error (%) HOS-based method	Normalized Estimation Error (%) Conventional (FFT)method
30	0.027	0.1
20	0.057	1.00
10	0.32	10.16
5	0.5	32.10

Table 4.2Case#1 Normalized estimation error for HOS and FFT based methods.

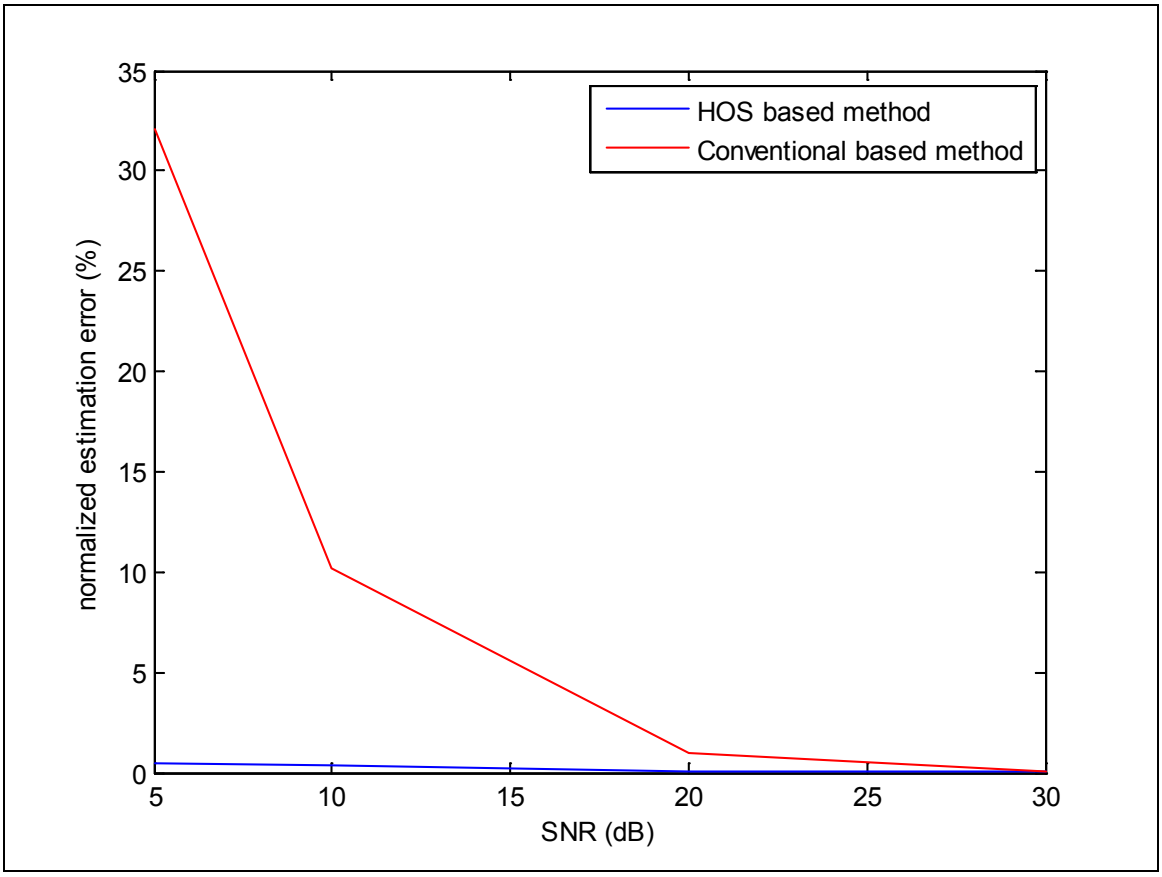

Figure 4.1:Normalized estimation error Vs. output's SNR using HOS and FFT based methods of new coating model (Gaussian noise).

From the results presented in Table 4.2 and Figure 4.1, it is clear that the normalized estimation error increases as the SNR reduces which is expected. Moreover, the performance of the HOS-based method is much better than the FFT based method such that the estimation error does not exceed 0.5% at 5dB while it is 32% in the case of FFT based method.

4.2 Case#2(The new coating model with noisy input/output (Gaussian noise):

In this part, both the input and output are distorted by additive Gaussian noise. The input's SNR is fixed at 10 dB while the output's SNR is changed so that the normalized estimation error is measured at different SNR values. The result of comparison is summarized in Table 4.3 and Figure 4.2:

SNR(dB)	Normalized Estimation Error (%) HOS-based method	Normalized Estimation Error (%) Conventional (FFT)method
30	0.05	13
20	0.19	17
10	0.34	22
5	1.5	52

Table 4.3Case#2 Normalized estimation errors for HOS and FFT based methods

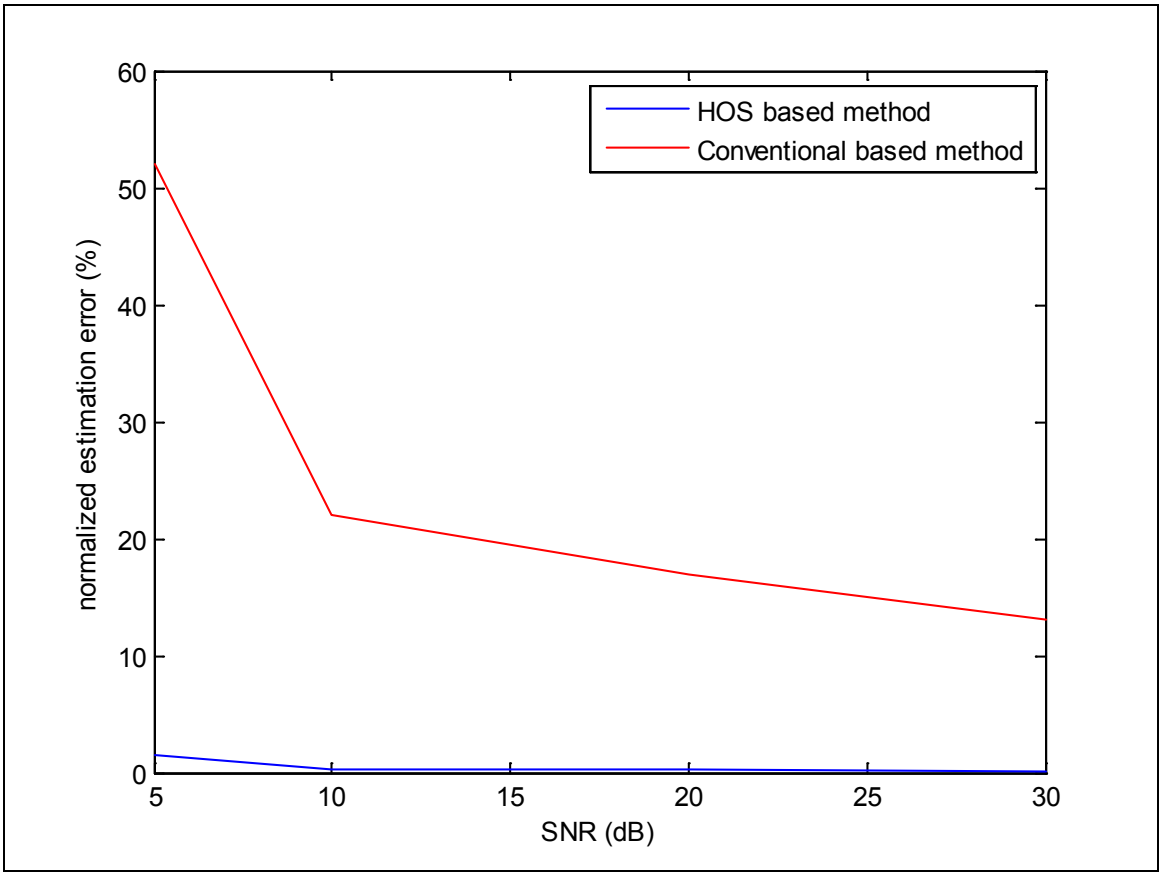

Figure 4.2Normalized estimation error Vs.output's SNR using HOS and FFT based methods of new coating model with input's SNR of 10 dB (Gaussian noise)

Although the case#2 result is similar to the findings presented in case #1, the gap between the performance of the FFT and HOS based method is much wider. This is because the ability of the HOS based method to eliminate the noise signals contaminating both the input and output data.

4.3 Case#3(The corroded coating model with noisy output (Gaussian noise):

Case #3 is similar to case #1 except that the system model represents a corrode coating. The result of comparison is summarized in Table 4.4 and Figure 4.3:

SNR(dB)	Normalized Estimation Error (%) HOS-based method	Normalized Estimation Error (%) Conventional (FFT)method
30	1.3	0.1
20	1.4	1
10	5.2	10
5	10	30

Table 4.4 Case#3 normalized estimation errors for HOS and FFT based methods

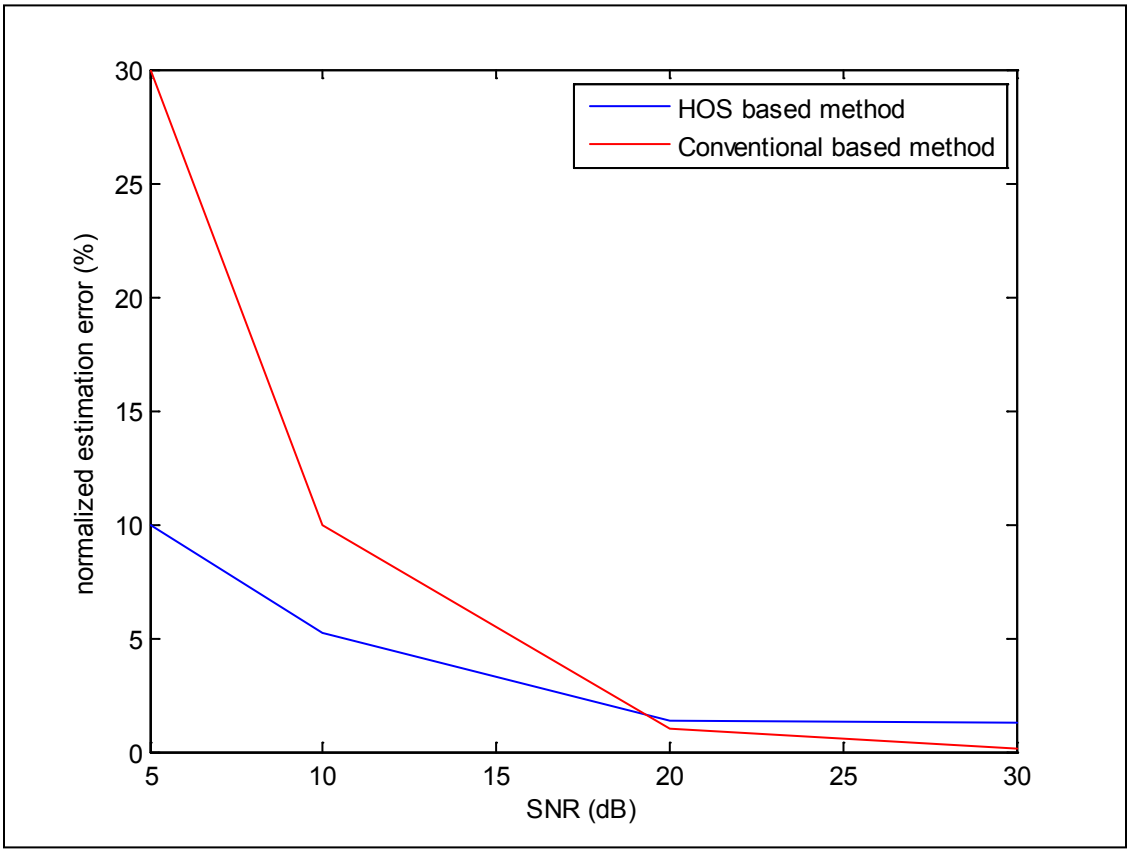

Figure 4.3:Normalized estimation error Vs.output's SNR using HOS and FFT based methods of bad coating model (Gaussian noise).

4.4Case#4(The corroded coating model with noisy input/output (Gaussian noise):

Case #4 is similar to case #2 except that the system model represents a corrode coating. The result of comparison is summarized in Table 4.5 and Figure 4.4:

SNR(dB)	Normalized Estimation Error (%) HOS-based method	Normalized Estimation Error (%) Conventional (FFT) method
30	1.6	10
20	1.9	12
10	7.2	22
5	12	46

Table 4.5Case#4 Normalized estimation errors for HOS and FFT based methods

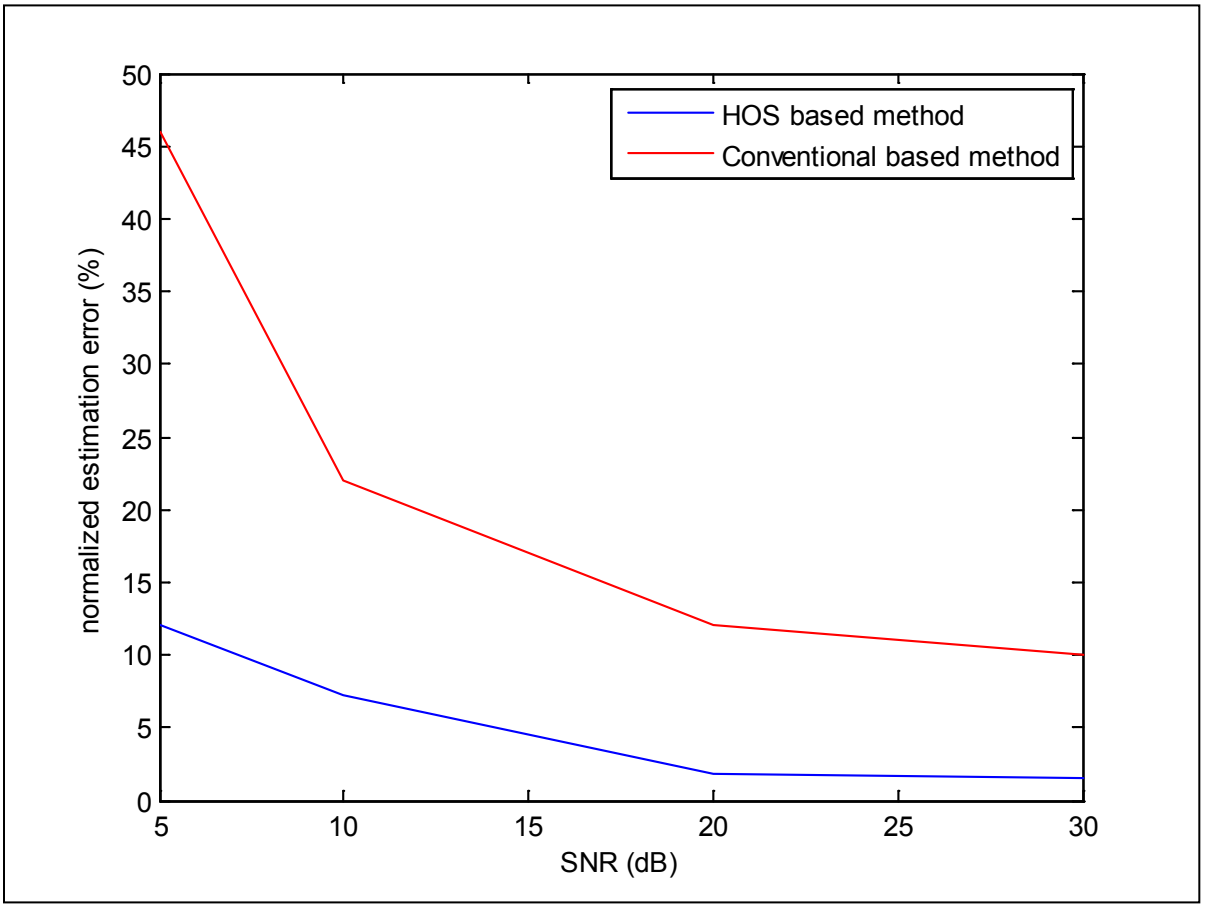

Figure 4.4: Normalized estimation error Vs.output's SNR using HOS and FFT based methods of bad coating model with input's SNR of 10 dB

As a result of the HOS and FFT-based methods comparison, it is cleared that the HOS-based method performs much better than the FFT-based method in the case of noisy measurements. The improvement in terms of estimation error reduction becomes more significant in the case of noisy input/output signals. This is related to the ability of HOS-based deconvolution method in estimating the impulse response in present of noisy input signals unlike the conventional deconvolution algorithms. Figures 4.5a (amplitude) and 4.5b (phase) show the estimated impedance spectrum using the HOS-based deconvolution with output's SNR of 20 dB (Case#1), while Figures 4.6a (amplitude) and 4.6b (phase) illustrate the estimated spectrum using the conventional method for the same output's SNR. Similarly, Figures 4.7 a, b and Figures 4.8 a, b show the impedance spectrum estimated by the HOS and FFT based methods respectively for input and output's SNR of 10 dB (Case#2).

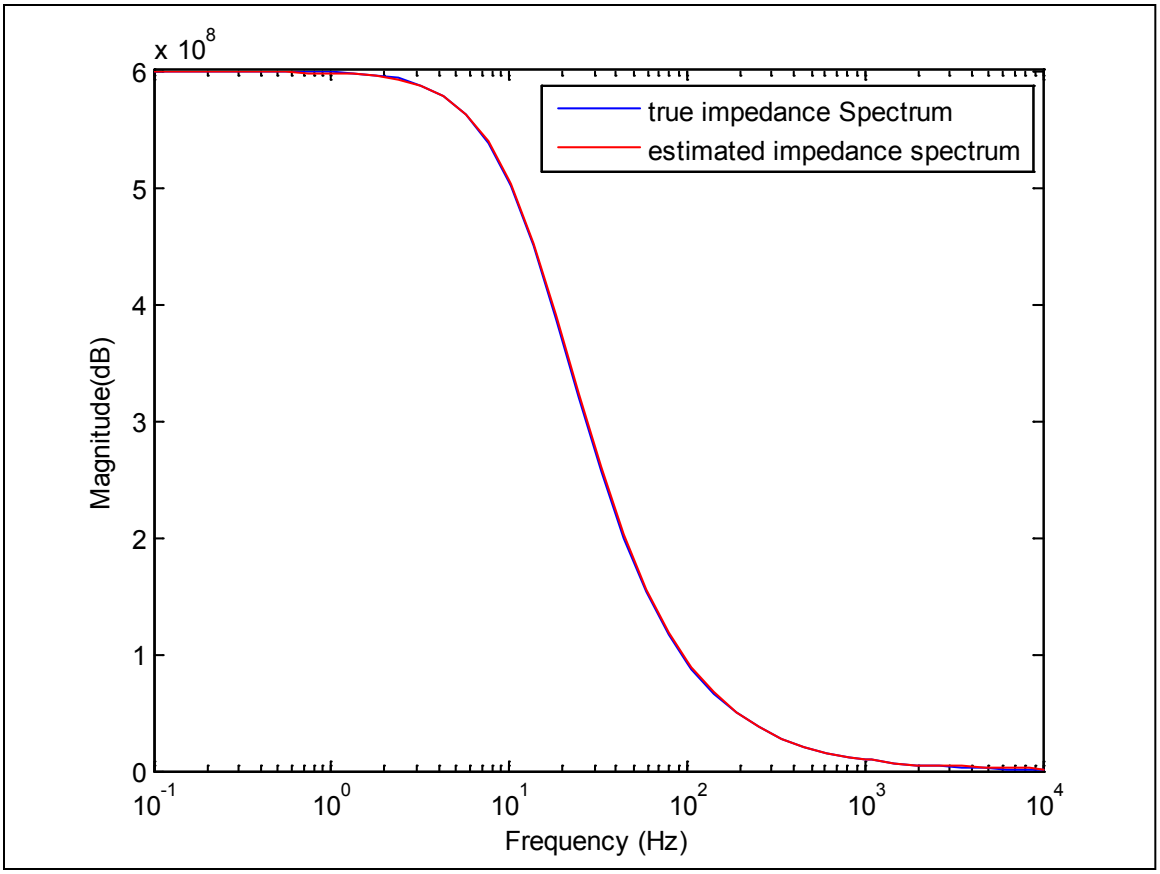

Figure 4.5a The true and estimated impedance spectrum (amplitude) using HOS-based method with output's SNR=20dB (Gaussian noise, case#1).

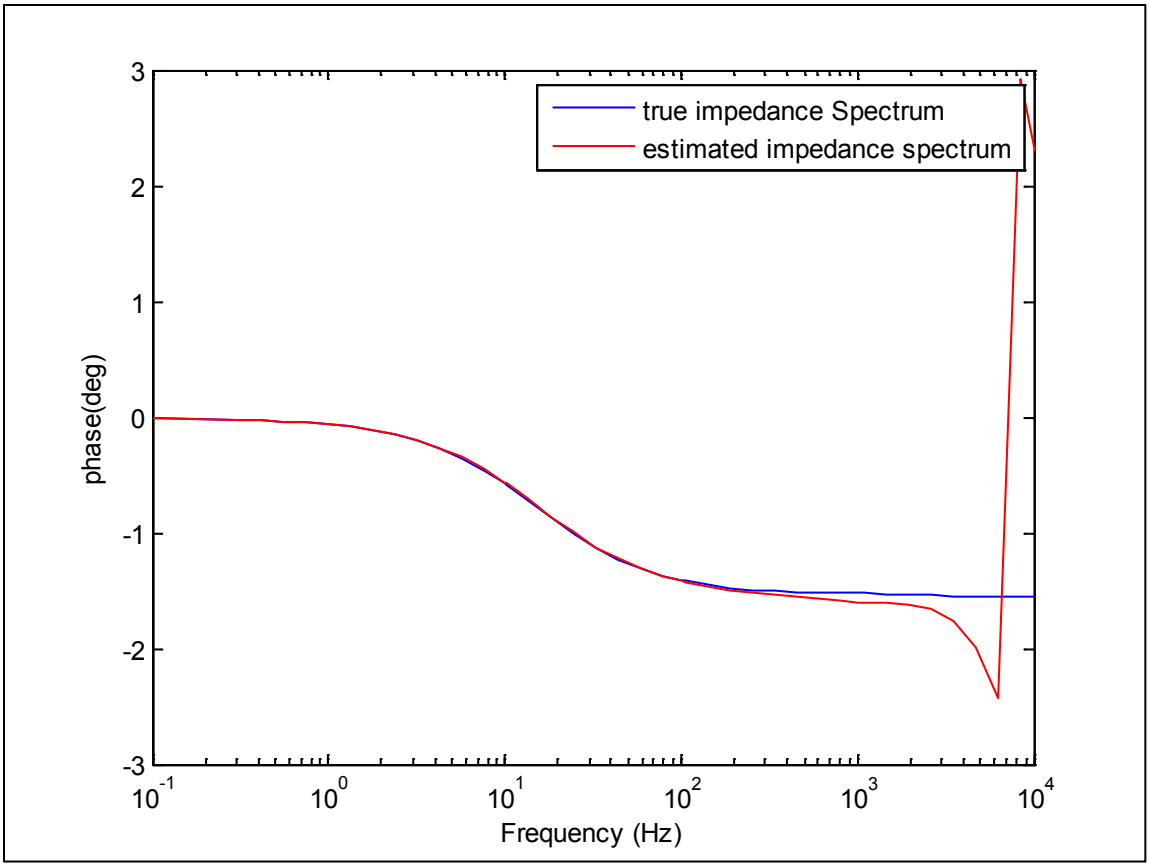

Figure 4.5b The true and estimated impedance spectrum (phase) using HOS-based method with output's SNR=20dB (Gaussian noise, case#1).

Figures 4.5 a, b show that the HOS-based deconvolution accurately estimates the impedance spectrum. However, for the phase part of the spectrum, there is a mismatch at the high frequency band and this is related to the frequency aliasing. This could be avoided by increasing the sampling rate and using bilinear transforms (Tustin approximation) for digital analog to conversion [43].

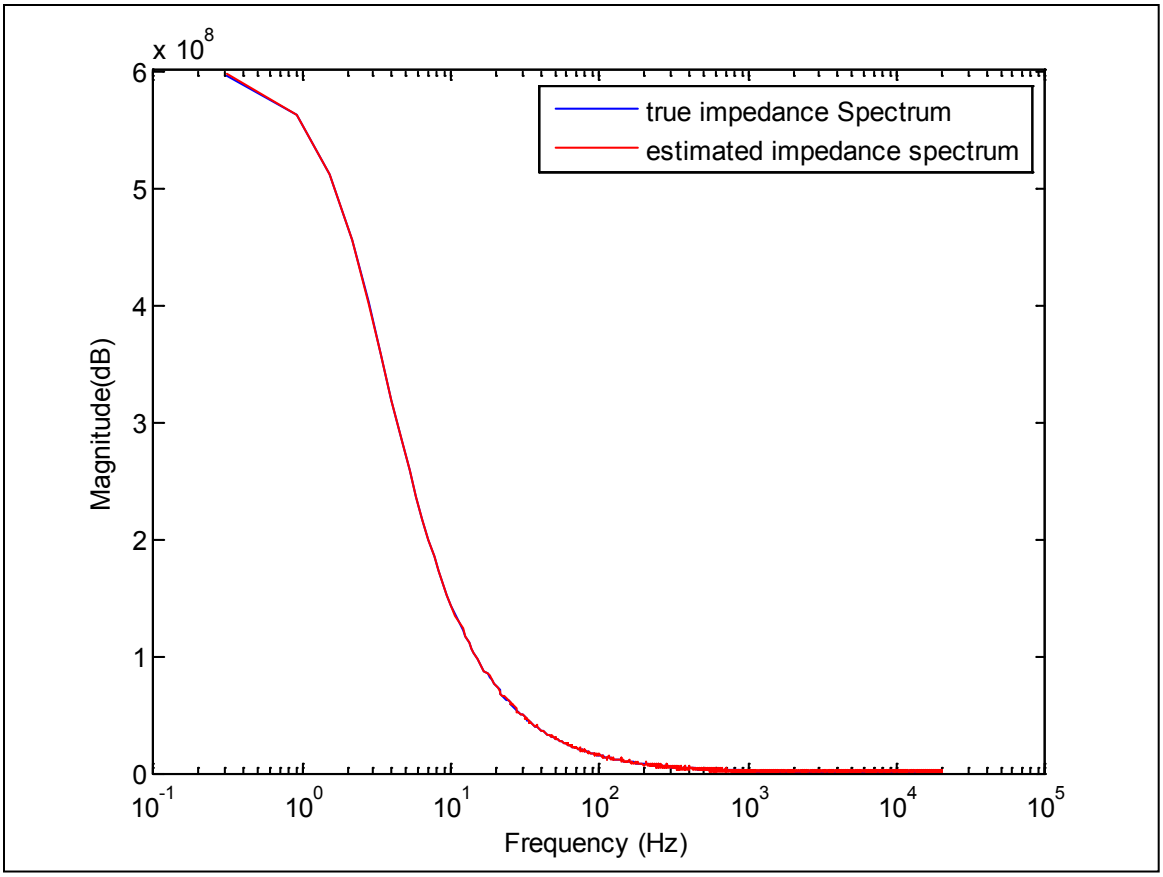

Figure 4.6a The true and estimated impedance spectrum (amplitude) using FFT-based method with output's SNR=20dB (Gaussian noise,case#1).

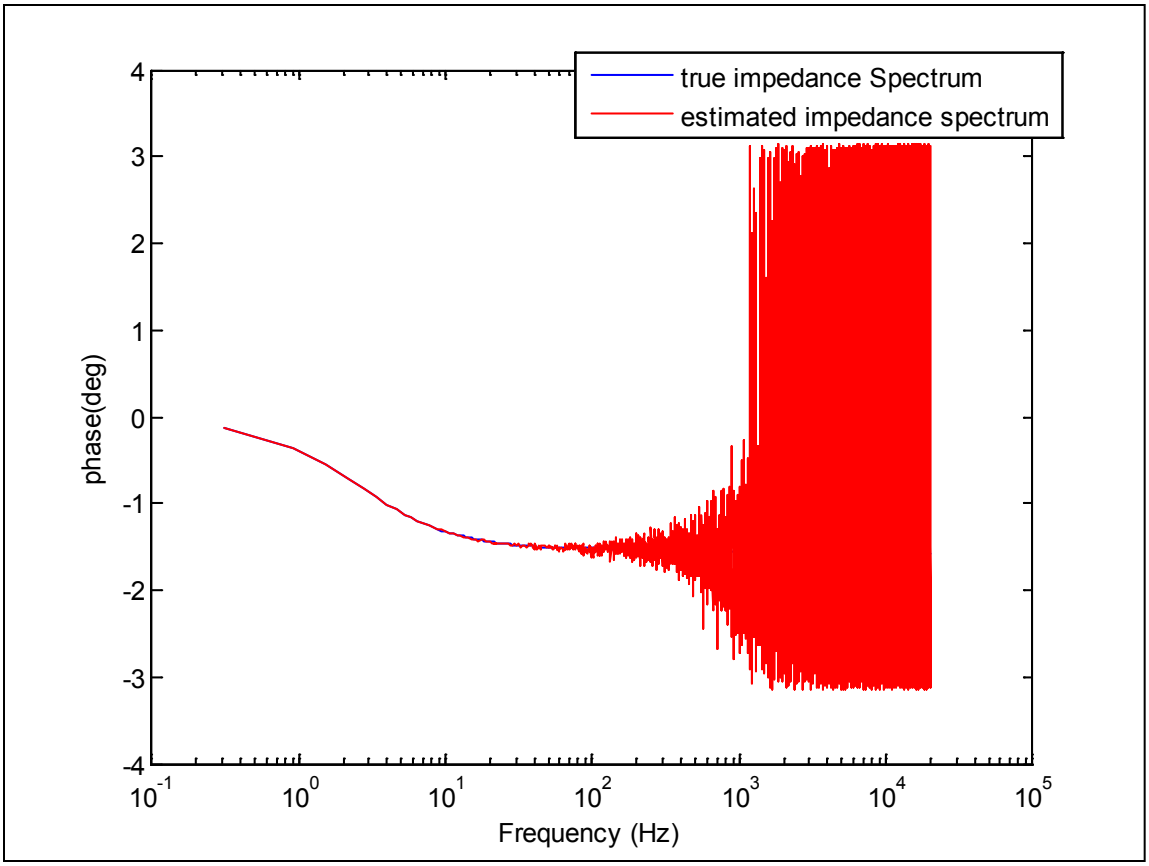

Figure 4.6bThe true and estimated impedance spectrum (phase) using FFT-based method with output's SNR=20dB (Gaussian noise, case#1).

As per Figures 4.6 b, the FFT based method does not produce an accurate impedance spectrum (phase part) even with moderate output's SNR (20dB).The phase mismatch happens clearly at the high frequency side.

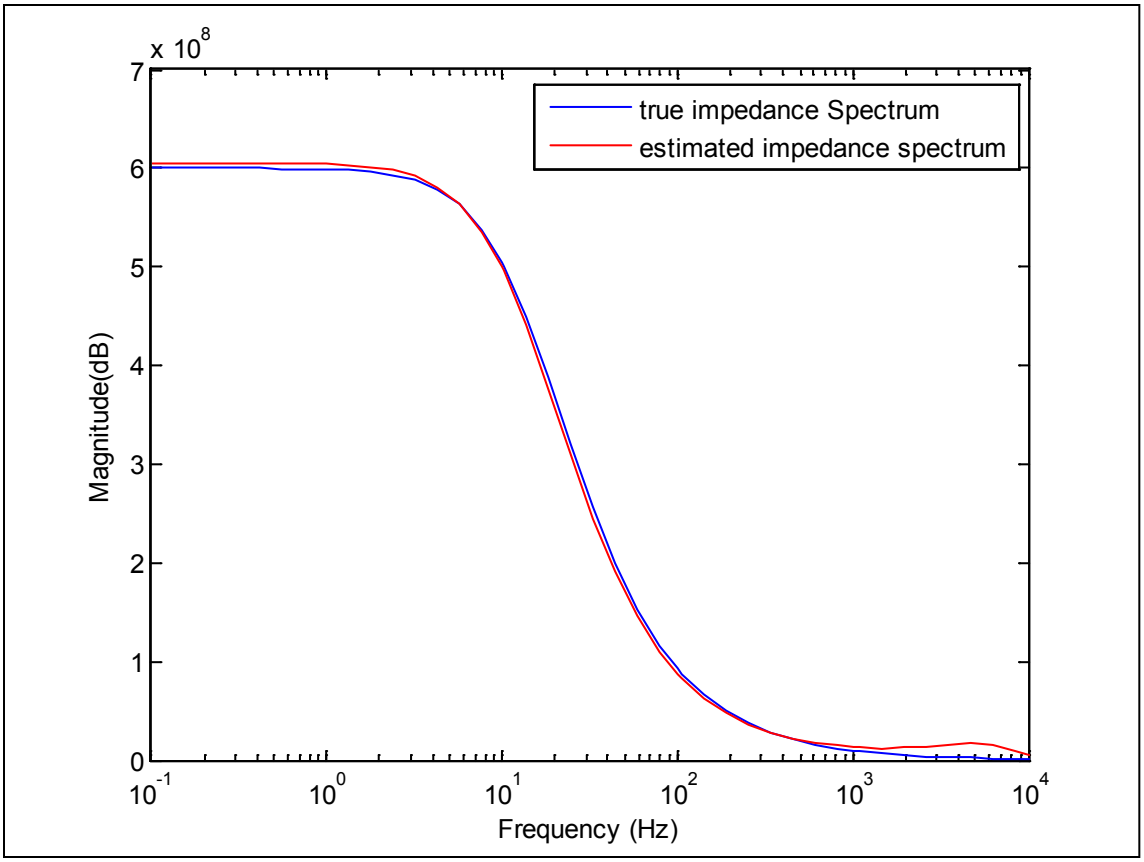

Figure 4.7a The true and estimated impedance spectrum (amplitude) using HOS-based method with output and input's SNR=10dB (Gaussian noise,case#2).

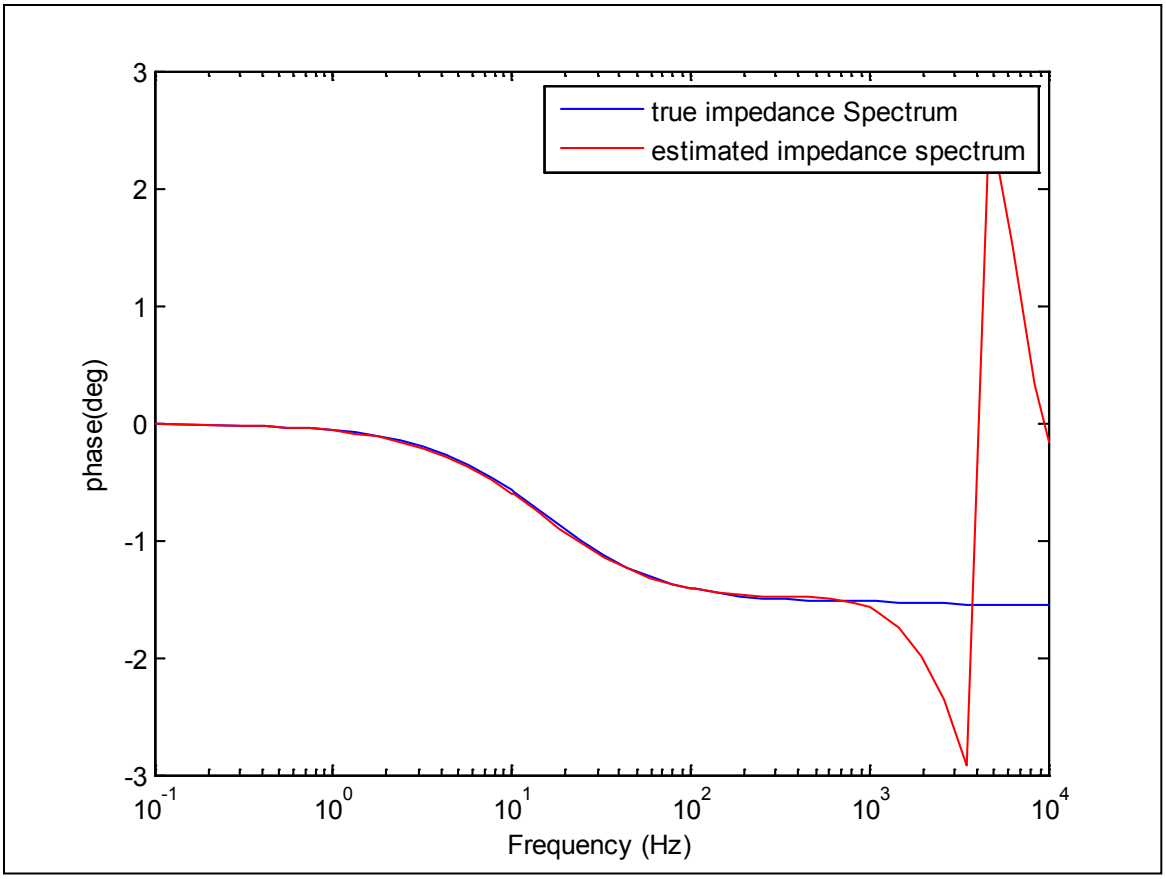

Figure 4.7b The true and estimated impedance spectrum (phase) using HOS-based method with output and input's SNR=10dB (Gaussian noise, case#2).

From the results presented in Figure 4.7a, b, it is obvious that the HOS based method is robust algorithm such that it measures the impedance spectrum precisely (amplitude and phase). The HOS-based method maintains the perfect performance even with low input and output's SNR (10dB). Note that, the high frequency band's mismatch is present here also and increasing the sampling frequency can eliminate it.

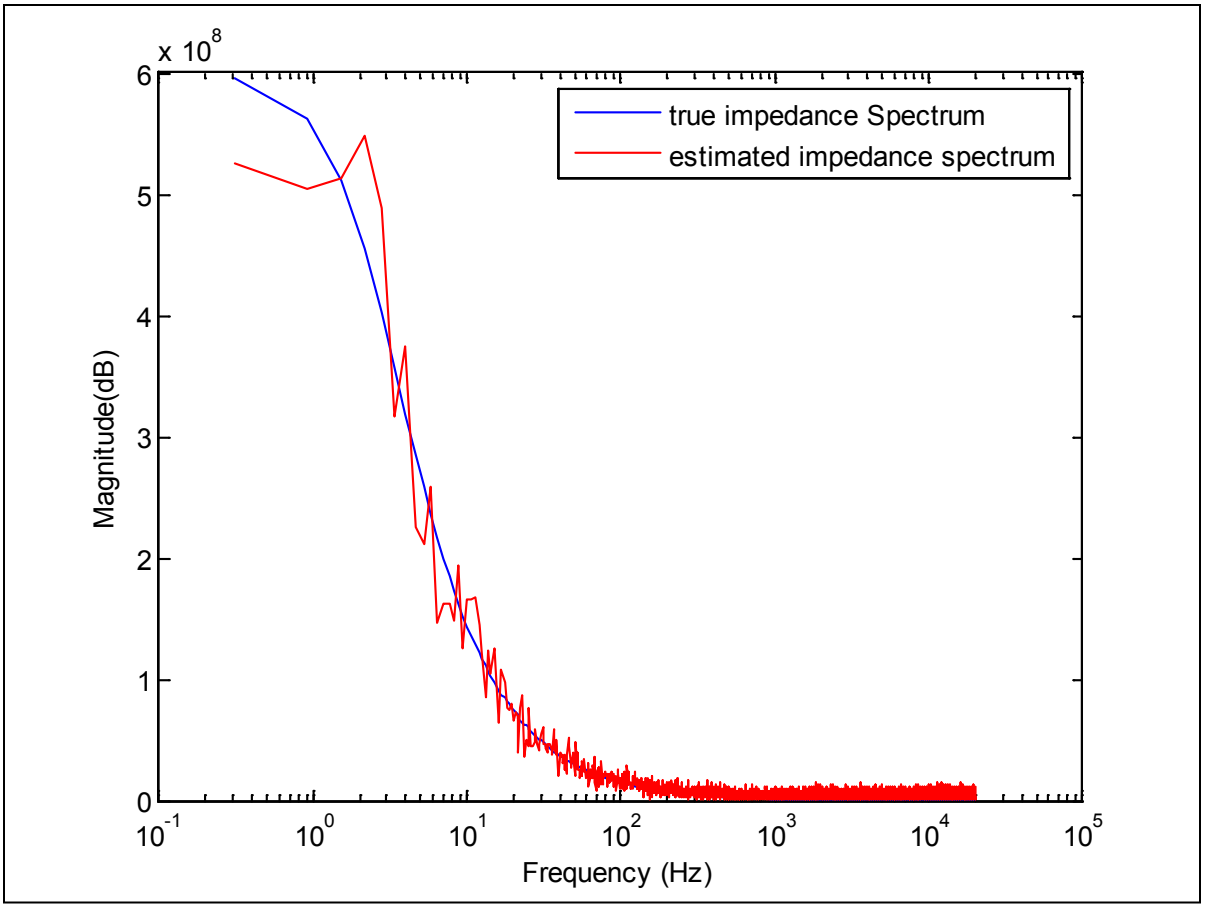

Figure 4.8a The true and estimated impedance spectrum (amplitude) using FFT-based method with input and output's SNR=10dB (Gaussian noise, case#2).

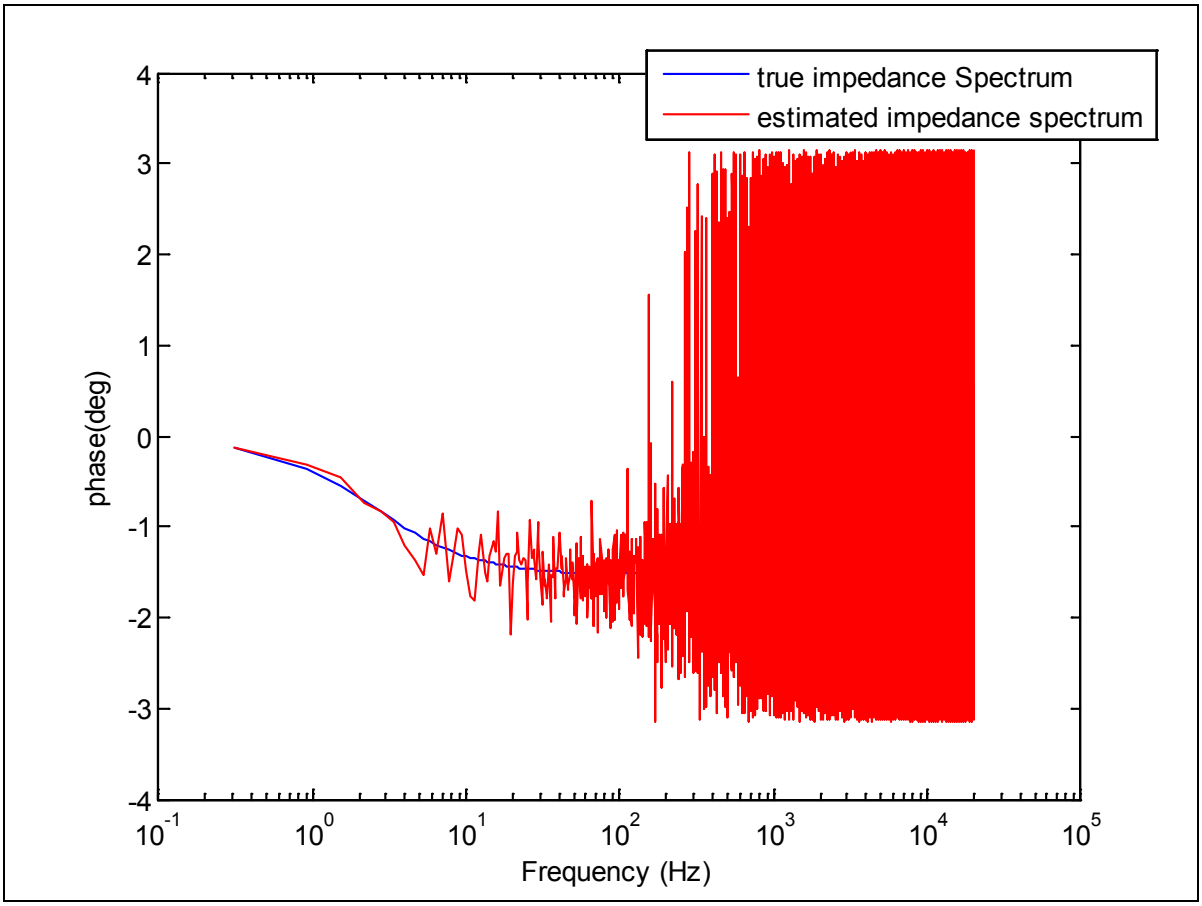

Figure 4.8b The true and estimated impedance spectrum (phase) using FFT-based method with input and output's SNR=10dB (Gaussian noise, case#2).

As per Figures 4.8a, b and unlike the HOS based method, the FFT based method is intensely affected by the noise interference signals in the case of low input and output's SNR(10dB). This is clear at the amplitude and phase parts of the impedance spectrum.

Forhigh output's SNR values, the estimation improvement using HOS-based method is clear at the phase part of the spectrum. However, for the week SNR values, the

improvement will occur both in the amplitude and phase spectrum as shown in Figures 4.7a,b and 4.8a,b.

Another observation form the result is that the HOS based deconvolution performs better in the case of new coating model compared with the corroded coating model. In the former, the normalized estimation error reaches 0.5% in the case of noisy output data while for the later; the normalized estimation error is 10%. Actually, the frequency band of the impedance spectrum and the applied signal (input) play role in this performance dissimilarity. The frequency spectrum of the impedance representing the corroded coating is wider (Maximum frequency $\approx$16000 Hz) than the one representing the new coating (Maximum frequency $\approx$1600 Hz) as shown in Figure 4.9. During the simulation, the applied signal is identical for the two cases, which is a short rectangle shaped pulse with frequency spectrum shown in the Figure 4.10. In order to have a better estimation performance, the frequency band of the applied signal should be as wide as the impedance spectrum or even more.

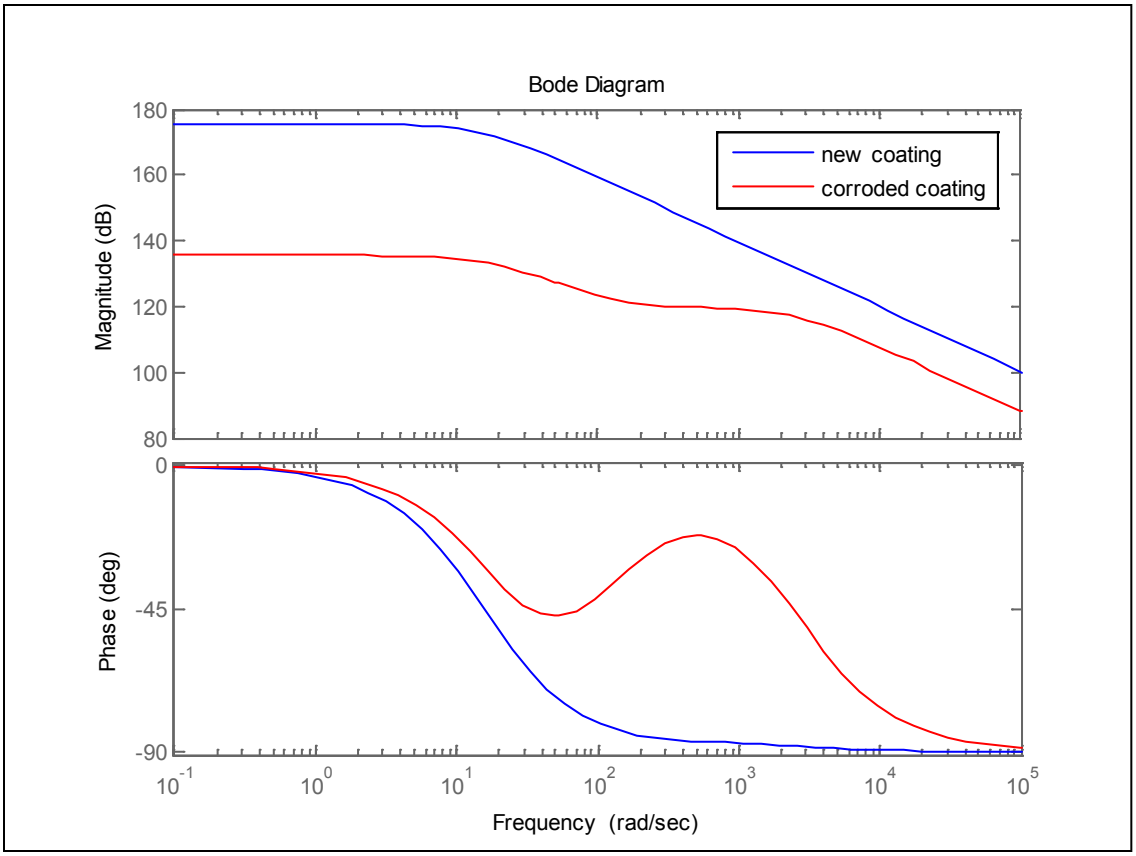

Figure 4.9The bode diagram for the new and corroded coating model

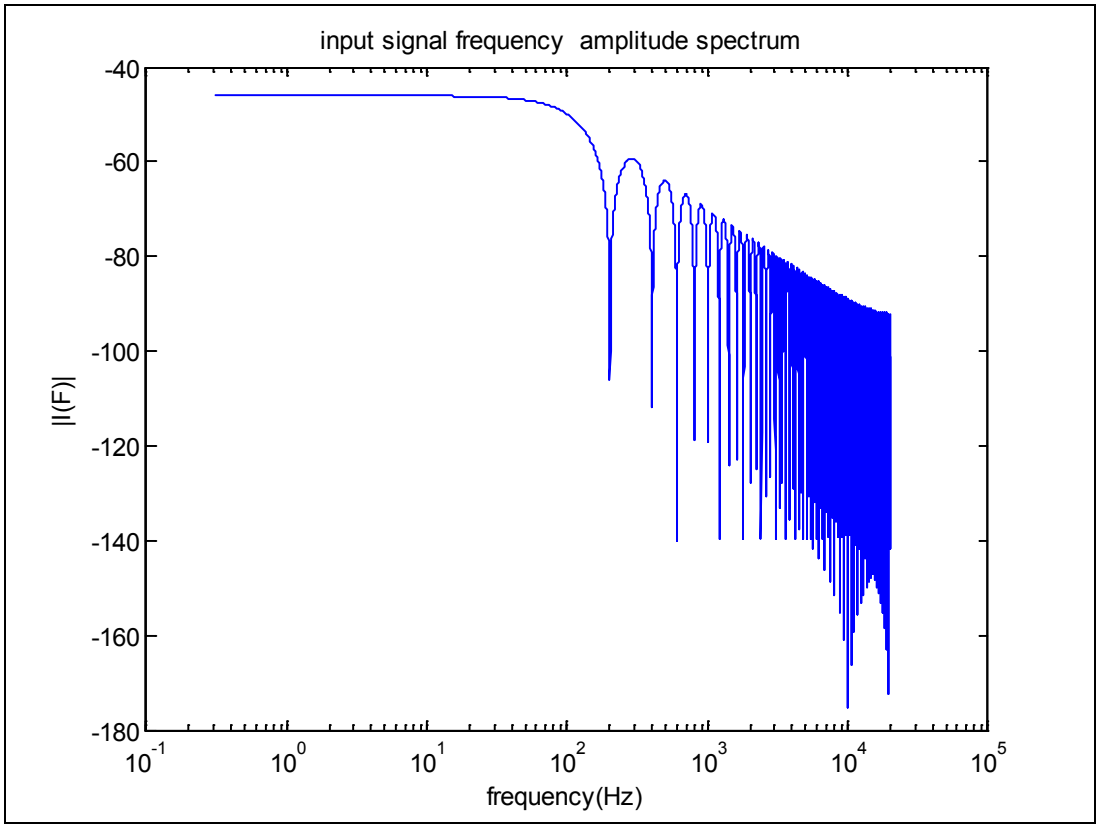

Figure 4.10The amplitude frequency response of a short rectangle pulse (the input signal)

4.5 Factors Affecting the Performance of HOS-based EIS Measurements:

In order to achieve a better estimation performance the frequency spectrum of the input signal needs to be wide as possible. At the same time, the third order moment of the input signal should not equal zero. In other words, the applied signal has to be non-Gaussian signal with a wider bandwidth. However, there is a contradiction between the two properties. This means that as the signal becomes non-Gaussian, its frequency bandwidth becomes narrower. To see the effect of the third order momentson the performance of the HOS based method, consider the following input signal used as applied signal to estimate the impedance spectrum of the new coating model:

$$i=10\exp(-t/0.05)^{n} \tag{4-2}$$

As the power (n) increases, the signals becomes narrower in the time domain which expands the frequency spectrum of the signals and reduces the 3rd order moments as shown in Figure 4.11 andTable 4.6.

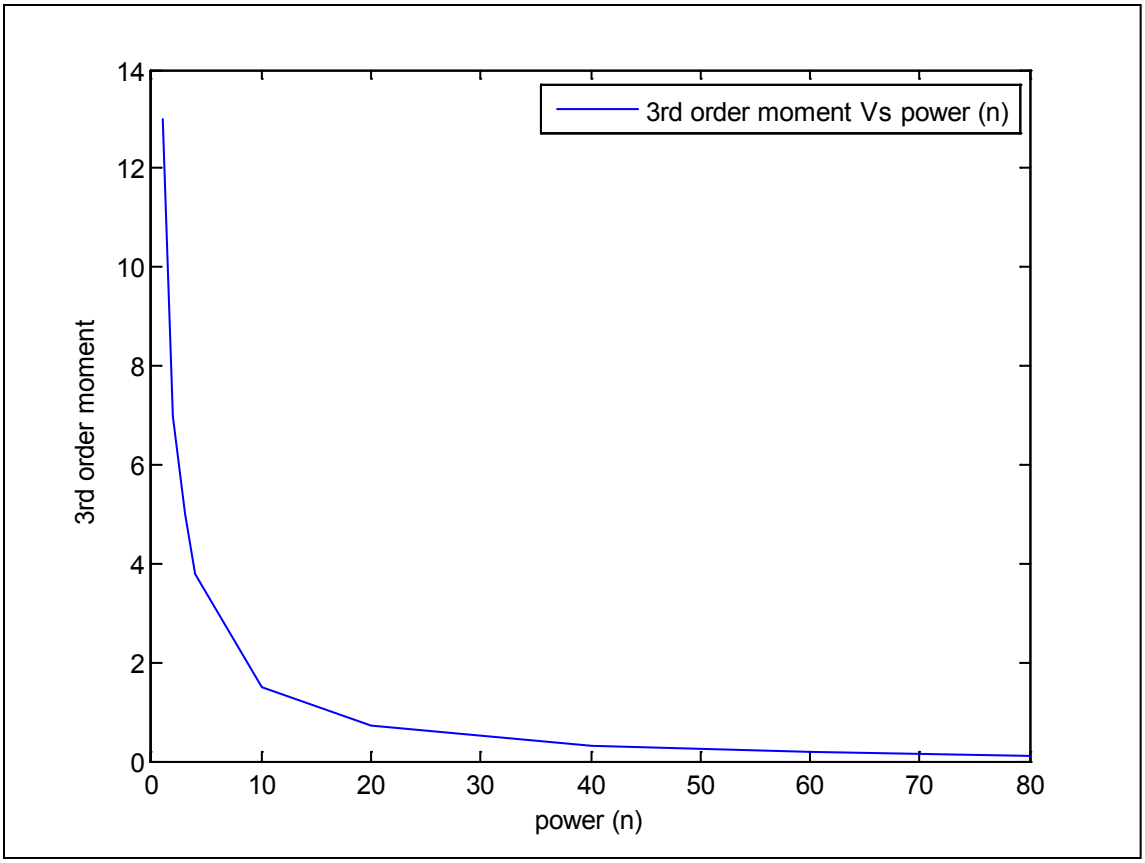

Figure 4.11: 3rd order moment Vs. the power (n) for the applied signal, $i=10\exp(-t/0.05)^n$

Power (n)	Cutoff Frequency (Hz)	3rd order Moment	Normalized estimation error (%)
1	1	13	0.2
2	2	7	0.1
3	3	5	0.07
4	4	3.8	0.005
10	10	1.5	0.1
20	20	0.7	0.8
40	30	0.3	1.6
60	40	0.2	3.6
80	60	0.1	5

Table 4.6: The normalized estimation error Vs. the input signal's 3rd order moment.

As per Figure 4.11 and Table 4.6, the power (n) manipulates the precision of the HOS-based method and by increasing the power (n), the estimation error decreases until the 3rd order moments reaches zero. At this point, the HOS-based method becomes inapplicable and the estimation error increase dramatically.So, in order to estimate the impedance spectrum properly, the 3rd order moment of the applied signal should be greater than zero.

It is noticed also that the assumed order of the nominator and dominator ($n_{a,}n_b$) of the impedance spectrum, which should be defined in the algorithm, could affect the performance of the estimation. When the assumed system's order is greater than the true model's order, the normalized estimation error reduces. Consider case#1 when the new coating model is estimated with noisy output data. While the true system order is (2, 3), theassumed order isvaried to see the effect on the estimation error and the result is summarized in Table 4.7:

Order ($n_{a,}n_b$)	Normalized estimation error (%)
(2,2)	0.1237
(3,3)	0.1178
(4,4)	0.0701
(5,5)	0.0710
(6,6)	0.0632

Table 4.7: The normalized estimation error Vs. the assumed system order ($n_{a,}n_b$).

Another factor influences the deconvolution precision is the cumulants maximum lag 'M' which should be specified in the cost function (3.16) [30,31]. The parameter M is selected between 50 and 100 and the following estimation error produced:

Parameter (M)	Normalized estimation error (%)
50	2.43
70	0.2615
90	0.1
100	0.08
200	0.04
300	0.02
400	0.03
500	0.04
600	0.04
1000	0.05

Table 4.8: The normalized estimation error Vs. the cumulant maximum lag, parameter M

From the result, the estimation error reduces as the parameter "M" increase until M =400 where the error starts to increase. This relation is identical to the findings obtained in reference [30]. There are region in which the parameter "M" gives best estimation results and it depends on the system and experiment conditions (empirical determination) .

The final goal of the EIS measurement is estimating the parameters of the equivalent circuit model representing electrochemical system. The HOS-based method estimates circuits' parameters more accurate compared with the FFT based method. This is because the error associated with the estimated impedance spectrum propagates to the estimation of the circuit parameters. To prove this outcome, LEVM (complex nonlinear least square curve fitting program) software [33], is used to estimate the parameters of the circuit representing the bad coating model. The inputs of the LEVM program are the impedance spectrum estimated by HOS and FFT-based methods (case#4 input and output's SNR=10 dB). The result is shown in Table 4.11.

parameter	Estimation error (%) HOS-based method	Estimation error (%) Conventional (FFT) method
R1(1e6Ω)	2	4
R2(5e6Ω)	1	2
C1(400e-12F)	2	5
C2(10e-9F)	9	14

Table 4.9 The estimation error of equivalent circuit parameters estimated by the HOS and FFT based method.

So, it is clear from Table 4.11 that the HOS based method is lower in parameter estimation error compared with the FFT method. The improvement here is about 50% reduction in the estimation error.

4.6 Performance of the HOS-based deconvolution in the case of non-Gaussian noise:

In addition of the additive Gaussian noise scenarios, the behavior of the HOS-based deconvolution is tested for non-Gaussian distribution noises (Uniform and Rayleigh). Table 4.9 shows the measured estimation error for approximating the impedance spectrum of the new coating model in the case of noisy output (Gaussian, Uniform and Rayleigh). In Table 4.10, a noisy input is also considered. The results show that the HOS-based method is robust in both the Gaussian and non-Gaussian noise distortion. HOS-based method has perfect performance in the case of Gaussian and Uniform noise than the Rayleigh noise. The similarity in the Gaussian and Uniform noise cases relates to the fact that they both have symmetric distribution with zero 3rd order moments.

SNR (dB)	Estimation error (%) (Gaussian)	Estimation error (%) (Uniform)	Estimation error (%) (Rayleigh)
30	0.02	0.01	0.01
20	0.05	0.03	0.02
10	0.3	0.2	0.4
5	0.5	0.9	1

Table 4.10 Estimation errors Vs. output's SNR at different noise distributions using HOS-based EIS for new coating model.

SNR (dB)	Estimation error (%) (Gaussian)	Estimation error (%) (Uniform)	Estimation error (%) (Rayleigh)
30	0.05	0.02	0.1
20	0.1	0.1	0.2
10	0.3	0.2	0.7
5	1	1	2

Table 4.11 Estimation error Vs. output's SNR at different noise distributions using HOS-based EIS for new coating model with input's SNR=10 dB.

4.7Discussions and Conclusions:

In this chapter, HOS (3rd Order Cumulants) Deconvolution based method used for EIS measurement is proposed. A comparison is done between the proposed method and the conventional FFT based method in estimating the impedance spectrum of a new and corroded coating metal model. The comparison is measured in terms of normalized estimation error considering additive Gaussian noise which distorts either the output signal only or both the input and output signals. A MATLAB program simulates the experiment and the following points are the main results of the test:

1. The HOS-based method estimates the impedance spectrum with lower estimation error compared with the FFT based method.
2. When both the input and output signals are contaminated by additive Gaussian noise, the improvement in the estimation precision using the HOS-based method is much clear.
3. A proper selection of the applied signal is required such that the third order moment of the signal should be greater than zero. In addition, the frequency spectrum of the input signal needs to be as wide as possible.
4. When the assumed model's orders are greater than the true model's order, the normalized estimation error starts reduce.

5. There are regions in which the cumulants maximum lag “M” gives best estimation results and it depends on the system and experiment conditions (empirical determination).
6. The HOS-based method is robust algorithmfor both Gaussian and non-Gaussian noise distributions.
7. HOS-based method has perfect performance in the case of Gaussian and Uniform noise compared with the Rayleigh noise.
8. Using the direct approach in estimating the frequency spectrum using digital to continuous transfer function conversation rather than using the FFT method gives better results. This direct method does not require any amplitude modification of the estimated frequency spectrum.
9. The HOS-based method estimates parameters of the equivalent circuit representing the coated metal more precisely compared with the FFT based method. The improvement is about 50% reduction of the normalized estimation error.
10. Although there is a big gap between the performance of the HOS-based and FFT based methods in estimating the impedance spectrum. The estimated circuit parameters using the two methods are similar in some cases. This happens when the level of the noise is low. The reason of this similarity is

theability of LEVM software in filtering out the noise by matching the output data to the required impedance spectrum.

The second part of this thesis focuses on the second step in the EIS, which is finding the circuit model's parameters. The CNLS estimates the circuit parameters using curve fitting of the EIS data produced either by FFT or FRA [34-38],[42]. There is possibility to find directly the circuit parameters in a noisy environment by one step. This can be achieved using a suitable adaptive filtering technique with a proper cost function in terms of the current and voltage across the tested system. This is discussed in detail in the next chapter.

CHAPTER 5

ADAPTIVE FILTERING

In the case of the HOS deconvolution, the electrochemical system's components are obtained indirectly. The frequency response is measured followed by the components estimation using the curve fitting techniques. On the other hand, using different adaptive filtering techniques (least square and steepest Descent) can give a direct estimation of the system's components. This could be accomplished by building the cost function in terms of the circuit's parameters: R_S, R_{po}, R_{ct} ,C_C and C_{dl},. In this section, a combination of least square and steepest descent adaptive filtering is used.

Adaptive filters are systems that react to variations in their environment by adapting their internal structure in order to meet certain performance specifications. It is considered as optimization tool that could be used to estimate specific variables in a noisy environment.

The adaptive filtering systems are widely used in communications, signal processing and control.

The applications of the adaptive filtering are found in many areas. For example, it is used in signal processing applications such as noise cancellation, deconvolution and adaptive beam forming. The telecommunication application includes channel equalization, channel estimation and echo cancelation. Moreover, adaptive filtering systems are utilized in control system applications for inverse control systems, active control of sound / Vibration and elimination of plant disturbance.

One of the main adaptive filtering applications is the channel estimation in which the channel properties in term of fading, scattering and power attenuation are defined. The main objective of the electrochemical impedance spectroscopy is to determine the impedance spectrum which could be treated as channel. So, there is possibility to apply adaptive filtering techniques in order to estimate the impedance spectrum. The two main AF techniques (Least Squares and Steepest Descent), which are used in proposed AF-based EIS, are explained briefly in the next sections.

5.1 Least Squares

If there is an (n × 1) vector y and (n× m) observation matrix H, the least squares problem looks for (m×1) weight vector w that solves the following cost function [39]:

$$\min_{w} \left\| y - Hw \right\|^2 \tag{5-1}$$

The solution of the above cost function (weight vector w) is unique if, and only if the column of data matrix H are linearly independent. This requires that the number of rows is greater than or equal the number of column (n ≥ m). By validating the above condition, the weight vector is given by:

$$w = (H^* H)^{-1} H^* y \tag{5-2}$$

In some cases, there are many solutions of the vector w when the product $H^* H$ is singular.

5.2 The Steepest Descent

The Steepest Descent [SD] is a method that will approximate the optimal solution of a linear estimator in iterative manner [39]. The need of the SD highlights when the optimal solution of linear estimation problem cannot be described in closed form.

Consider a zero-mean random variable d with variance σ_d^2, zero mean random row vector u and correlation matrix $R_u = Eu^* u > 0$. The solution of a linear least squares estimation problem:

$$\min_{w} E\left|d - uw\right|^2 \tag{5-3}$$

is given by the weight vector w:

$$w = R_u^{-1} R_{du}. \tag{5-4}$$

In this situation, the cost function is quadratic in w and it has a global minimum at w_o. However, in some cases, the correlation matrix R_u is not invertible and hence there is no closed form solution. The SD algorithm can determine the optimal solution (w) recursively with initial guess w_{-1}:

$$w_i = w_{i-1} + \mu p, \quad i \geq 0 \tag{5-5}$$

μ is the step size and p is the update direction vector which equals the gradient of the cost function with respect to the weight vector:

$$p = -B\left[\nabla_w J(w_{i-1})\right]^*$$

$$J(w) = E\left|d - uw\right|^2 \tag{5-6}$$

In order to have a success estimation of the weight vector (w), the value of the step size μ should be in the region ($0 < \mu < 2/\ \lambda_{max}$). The ($\lambda_{max}$) is the maximum eigenvalue of the correlation matrix R_u. In addition and to insure the fastest converges of the solution, the step size μ should equal $2/(\lambda_{max} + \lambda_{min})$, where λ_{min} represents the smallest eigenvalue of the correlation matrix R_u.

5.3 EIS measurement using Adaptive Filtering Algorithm

The main objective of EIS is to determine the frequency response of the impedance system. There is another approach of the previous objective which is finding directly the parameters of the equivalent circuit representing the impedance system. The adaptive filtering techniques could estimate these parameters by minimizing a pre-defined cost function in terms of the required circuit's parameters.

Consider the following simple RC circuit:

$$Z = R + jwC$$

Figure 5.1: RC circuit

If a galvanostaticmode is used in the analysis of the above circuit where a constant current is across this circuit applied at different frequencies, different output voltages are obtained. In this case, there will be two data vectors for the applied current and the output voltage, which are equivalent to the vectors y and H respectively used in

the Least Squares solution. As a result, the least square AF algorithm could estimate the parameters R and C by solving (5.1) using (5.2):

$$w = \begin{bmatrix} R \\ 1/c \end{bmatrix}$$

$$H = \begin{pmatrix} I_1 & -jI_1 \\ \vdots & \vdots \\ I_m & -jI_m \end{pmatrix}$$

$$y = \begin{bmatrix} v_1 \\ v_2 \\ * \\ * \end{bmatrix}$$

Where w is the circuit parameters (R&C),H is the current matrix at which the circuit is stimulated and y is the output voltage data.

The second model circuit, which can be analyzed using AF, is the circuit representing the Randles cell model shown in the Figure (5.2):

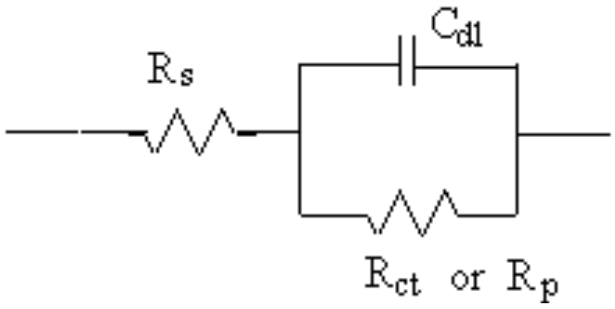

$$Z = R_s + \frac{R_{ct}}{1 + jwR_{ct}C_{dl}}$$

Figure 5.2: Randles Cell circuit model [41]

The Randles cell is one of the simplest and most common cell models. It includes a solution resistance (R_s), a double layer capacitor (C_{dl}) and a charge transfer or polarization resistance (R_{ct}, R_{po}). In addition to being a useful model in its own right, the Randles cell model is often the starting point for other more complex models.

For the Randles Cell model, the equivalent circuit impedance is not a linear combination of the parameters. So, the LS method cannot be utilized in this case. Alternatively, the Steepest Descent can be used with the following cost function:

$$J(Z) = E\left| V - IZ \right|^2 \tag{5-7}$$

while Z is the required impedance, V and I are the Z-transform of the voltage and current signals respectively.The solution of the cost function (5.7) is the recursive equation (5.5) and the weight vector is function of the circuit's parameter .To find the update direction vector P, a partial gradient of the cost function is calculated with respect of the circuit parameters as outlined below:

$$P = -[\nabla_{R1,R2,C1} J(v_{i-1} - I_{i-1} z_{i-1})]^* \tag{5-8}$$

$$P = -\begin{bmatrix} \frac{\delta J}{\delta e}\frac{\delta e}{\delta z}\frac{\delta z}{\delta R1} \\ \frac{\delta J}{\delta e}\frac{\delta e}{\delta z}\frac{\delta z}{\delta R2} \\ \frac{\delta J}{\delta e}\frac{\delta e}{\delta z}\frac{\delta z}{\delta C1} \end{bmatrix}^* \tag{5.9}$$

$$\frac{\delta J}{\delta e} = Le^* \mid e \mid^{2(L-1)} = e^* \tag{5-10}$$

Where, L=1 for the mean square error optimization and the error (e) equals the cost function (5.7)

$$\frac{\delta e}{\delta z} = -I \tag{5-11}$$

$$\frac{\delta z}{\delta R1} = 1 \tag{5-12}$$

$$\frac{\delta z}{\delta R2} = \frac{1}{(1 + jwC_1R_2)^2} \tag{5-13}$$

$$\frac{\delta z}{\delta C1} = \frac{-jR2^2}{(1 + jwC1R2)^2} \tag{5-14}$$

Finally, the following recursion equation estimates the circuit parameters R1, R2 and C1:

$$\begin{bmatrix} R1_i \\ R2_i \\ C1_i \end{bmatrix} = \begin{bmatrix} R1_{i-1} \\ R2_{i-1} \\ C1_{i-1} \end{bmatrix} + \mu(V_{i-1} - I_{i-1}Z_{i-1})I^*_{i-1} \begin{bmatrix} \frac{\delta z_{i-1}}{\delta R1_{i-1}} \\ \frac{\delta z_{i-1}}{\delta R2_{i-1}} \\ \frac{\delta z_{i-1}}{\delta C1_{i-1}} \end{bmatrix}^* \tag{5-15}$$

The parameters of the circuit representing the coated metal (Figure 3.3) are estimated by the same SD algorithm used for the Randles cell model. The recursion equation estimates the circuit parametersof the coated metal is:

$$\begin{bmatrix} Rs_i \\ Rpo_i \\ Rct_i \\ Cc_i \\ Cdl_i \end{bmatrix} = \begin{bmatrix} Rs_{i-1} \\ Rpo_{i-1} \\ Rct_{i-1} \\ Cc_{i-1} \\ Cdl_{i-1} \end{bmatrix} + \mu(v_{i-1} - z_{i-1} I_{i-1}) I_i \begin{bmatrix} \frac{\delta z_{i-1}}{\delta Rs_{i-1}}^* \\ \frac{\delta z_{i-1}}{\delta Rpo_{i-1}}^* \\ \frac{\delta z_{i-1}}{\delta Rct_{i-1}}^* \\ \frac{\delta z_{i-1}}{\delta Cc_{i-1}}^* \\ \frac{\delta z_{i-1}}{\delta Cdl_{i-1}}^* \end{bmatrix} \quad (5\text{-}16)$$

CHAPTER 6

PERFORMANCES of EIS ADAPTIVE FILTERING BASED METHOD (SIMULATION RESULT)

In this chapter, the performance of the AF based method is examined in terms of the normalized error of the estimated parameters. A MATLAB program simulates a galvonostatice mode test where a constant current (frequency domain) is applied to the electrochemical cell producing output voltage. In order to measure the robustness of the AF algorithms, a noise signals are added to both the input and output signals with either Gaussian or non-Gaussian distribution. The test is done for both Randles cell as well as coated metal models.

6.1 Randles Cell model

A dummy Randles cell model is selected with the following parameters:

Parameter	Value
R1(solution resistance)	10Ω
R2(Polarization resistance)	100Ω
C1(double layer capacitance)	100e-6 F

Table 6.1: Randles Cell's Parameters.

In this test, two different cases for each noise distribution is made such that in case#1, the noise is introduced in the output side only, While in case #2, the noise was added at the input (fixed at 20 dB) and output sides. As explained in chapter 5.2, a SD algorithm is utilized for the parameter estimation for the Randles model.

6.1.1 Case #1 (The Randles Cell model with noisy output (Gaussian noise) :

At the beginning, it is noticed that the SD algorithm gives an accurate estimate for R1. However, the estimation for the other parameters (R2&C1) is imperfect. In order to take the advantage of the R1 estimation, the LS method is used after the voltage contribution of R1 is removed fromthe voltage output data. This means that a voltage division rule is utilized to get the voltage dropped across the parallel section of the

circuit (R2, C1). After that and since the LS circuit is suitable for the series circuit configuration, the LS method will estimate the admittance instead of the impedance according to the new voltage data resulted from the voltage division. Table 6.2 shows the result of the circuit estimation:

	R1		R2		C1	
SNR(dB)	Estimated Value(Ω)	Estimation error (%)	Estimated Value(Ω)	Estimation error (%)	Estimated Value(F)	Estimation error (%)
20	10	0	99	1	47e-6	53
10	10	0	101	1	6.1e-6	100
5	10	0	113.6	13.6	0.2e-6	100

Table 6.2 The estimated values and estimation error of the Randles Cell's parameters Vs. output's SNR.

The result shows accurate R1 estimation while the precision for the other parameters decreases as the SNR increases. Fortunately, the accuracy of R2&C1 could be improved if they are estimated at the low frequency band of the spectrum (see Table 6.3).

SNR(dB)	Frequency bandwidth included in the test (Hz)		
	1000	500	100
20	1.3	0.0%	0.0%
10	14%	4%	0.2%
5	33.2	12	0.9

Table 6.3 C1's Estimation error Vs. Frequency points processed for different SNR values.

In the low frequency side of the spectrum, there is a contribution of the parallel section of the circuit to the overall impedance. This is because the impedance of the capacitor (C1) is very large at the low frequency band and it decrease as the frequency increases. At the high frequency part of the spectrum, the R1 is the dominant part of the circuit.

Table 6.4 shows the final result of the AF algorithm in estimating the circuit parameters of the Randles cell model after implementing the following modification steps:

1. Applying SD algorithm to estimate the R1 while using LS algorithm to estimate the R2 and C1. The LS method will be used after getting the voltage dropped across the parallel section of the circuit based on the estimated value of the R1.
2. While R2 and C1 are estimated at the low frequency band of the spectrum, the data measured at the full frequency spectrum is considered for estimating R1.

	R1		R2		C1	
SNR(dB)	Estimated Value(Ω)	Estimation error (%)	Estimated Value(Ω)	Estimation error (%)	Estimated Value(F)	Estimation error (%)
20	10	0	100	0	100e-6	0
10	10	0	101	1	99.8e-6	0.2
5	10	0	101	1	98	2

Table 6.4 The estimated values and estimation error of the Randles Cell's parameters Vs. output's SNR(Gaussian noise).

6.1.2 Case #2 (The Randles Cell model with noisy input/output (Gaussian noise) :

The test's result is summarized in Table 6.5:

	R1		R2		C1	
SNR(dB)	Estimated Value(Ω)	Estimation error (%)	Estimated Value(Ω)	Estimation error (%)	Estimated Value(F)	Estimation error (%)
20	10	0	100	0	101e-6	1
10	10	0	101	1	102e-6	2
5	9	10	105	5	97e-6	3

Table 6.5The estimated values and estimation error of the Randles Cell's parameters Vs. output's SNR with input's SNR of 20 dB(Gaussian noise).

The result shows that AF based method is capable to estimate the Randles Cell's parameters directly with maximum estimation error of 2% with output's SNR of 5 dB. However, this performance is not met for noisy input/output data such that the minimum input SNR at which the AF-based method is operational is 20 dB while it is 10 dB for HOS-based method. In cases 3, 4, 5 and 6, Uniform and Rayleigh noise are considered to see the flexibility of the AF based method with different noise statistics.

6.1.3 Case #3 (The Randles Cell model with noisy output (Uniform noise) :

The test's resultis summarized in Table 6.6:

	R1		R2		C1	
SNR(dB)	Estimated Value(Ω)	Estimation error (%)	Estimated Value(Ω)	Estimation error (%)	Estimated Value(F)	Estimation error (%)
20	10	0	101	1	100e-6	0
10	10	0	101	1	97.4e-6	2.5
5	10	0	99	1	94e-6	6

Table 6.6 The estimated values and estimation error of the Randles Cell's parameters Vs. output's SNR(uniform noise).

6.1.4 Case #4 (The Randles Cell model with noisy input/output (uniform noise) :

The test's resultis summarized in Table 6.7:

	R1		R2		C1	
SNR(dB)	Estimated Value(Ω)	Estimation error (%)	Estimated Value(Ω)	Estimation error (%)	Estimated Value(F)	Estimation error (%)
20	10	0	101	1	99e-6	1
10	10	0	102	2	97e-6	3
5	12	20	106	6	88e-6	12

Table 6.7 The estimated values and estimation error of the Randles Cell's parameters Vs. output's SNR with input's SNR of 20 dB (uniform noise).

6.1.5 Case #5 (The Randles Cell model with noisy input (Rayleigh noise) :

The test's resultis summarized in Table 6.8:

	R1		R2		C1	
SNR(dB)	Estimated Value(Ω)	Estimation error (%)	Estimated Value(Ω)	Estimation error (%)	Estimated Value(F)	Estimation error (%)
20	11.6	16	98	2	103e-6	3
10	15	50	94	6	111e-6	11
5	19	90	89	11	120e-6	20

Table 6.8 The estimated values and estimation error of the Randles Cell's parameters Vs. output's SNR (Rayleigh noise).

6.1.6 Case #6 (The Randles Cell model with noisy input/output (Rayleigh noise) :

The test's resultis summarized in Table 6.9:

	R1		R2		C1	
SNR(dB)	Estimated Value(Ω)	Estimation error (%)	Estimated Value(Ω)	Estimation error (%)	Estimated Value(F)	Estimation error (%)
20	11	10	94	6	107e-6	7
10	15	5	91	9	86e-6	14
5	19	90	86	14	125e-6	25

Table 6.9 The estimated values and estimation error of the Randles Cell's parameters Vs. output's SNR withinput's SNR of 20 dB(Rayleigh noise).

For Uniform noise conditions, the estimation error is usually greater than estimation error resulted in the case of Gaussian noise signals. In addition, the AF could not estimate the circuit parameters with accepted accuracy figures in the case of Rayleigh noise signals.

6.2 Coated Metal Model:

In order to compare between the performances of the AF and the HOS-based methods, the same corroded coated model tested in chapter 4 is considered in this chapter. The AF estimation method consists of five main steps:

1. Applying the SD method to estimate the R1 (solution /electrolyte resistance).
2. A Voltage division tool is used to find the voltage dropped across the parallel section of the circuit followed by a LS method in order to estimate C1 (coating capacitor).
3. A current division algorithm is used to find the current passing through the (R2+R3//C2) section of the circuit.
4. Based on the current resulted from step#3, a SD method is applied to estimated R2 (polarization resistance).
5. Finally, the R3 (charge transferresistance) and C3 (double layer capacitance) are measured using the LS method in terms of admittance after the voltage across them is obtained by the voltage division rule.

Table 6.10 and 6.11 show the parameters' normalized estimation error for the noisy output and noisy input/output cases respectively with Gaussian distributions:

	R1		R2		C1		C2	
SNR (dB)	Estimated Value(Ω)	Estimation error (%)	Estimated Value(Ω)	Estimation error (%)	Estimated Value(F)	Estimation error (%)	Estimated Value(F)	Estimation error (%)
20	1.01e6	1	5e6	0	402e-12	0.5	10e-9	0
10	1.0e6	0	5e6	0	394e-12	1.5	9.9e-9	1
5	1.0e6	0	5.1e6	2	377e-12	6	9.9e-9	1

Table 6.10 The estimated values and estimation error of the Coated metal model's parameters Vs. output's SNR (Gaussian noise)

	R1		R2		C1		C2	
SNR (dB)	Estimated Value(Ω)	Estimation error (%)	Estimated Value(Ω)	Estimation error (%)	Estimated Value(F)	Estimation error (%)	Estimated Value(F)	Estimation error (%)
20	1.0e6	0	4.8e6	4	408e-12	2	10e-9	0
10	9.8e6	2	4.7e6	6	460e-12	15	10.3e-9	3
5	1.1e6	10	5.4e6	8	384e-12	4	9.1e-9	1

Table 6.11 The estimated values and estimation error of the Coated metal model's parameters Vs. output's SNR with input's SNR of 20 dB(Gaussian noise).

Tables 6.10 and 6.11 show that the AF –based method estimates directly the circuit's parameters of the coated metal with higher estimation error (6%) compared with Randles Cell model (2%). This is related to the number of steps involved in the coated metal estimation and the possibly of error propagation.

For the non-Gaussian noises distributions (Uniform & Rayleigh), it is noticed that, the performance is similar to the Gaussian case (see Tables 6.12 and 6.13). However, the AF based method does not estimate the circuit parameters adequately when the input is also disturbed by noise signals.

	R1		R2		C1		C2	
SNR (dB)	Estimated Value(Ω)	Estimation error (%)	Estimated Value(Ω)	Estimation error (%)	Estimated Value(F)	Estimation error (%)	Estimated Value(F)	Estimation error (%)
20	1.0e6	0	4.8e6	4	397e-12	1	10e-9	0
10	1.0e6	0	5.1e6	2	400e-12	0	9.9e-9	1
5	1.01e6	1	5.1e6	2	371e-12	7	9.9e-9	1

Table 6.12 The estimated values and estimation error of the coated metal model's parameters Vs. output's SNR (Uniform noise).

	R1		R2		C1		C2	
SNR (dB)	Estimated Value(Ω)	Estimation error (%)	Estimated Value(Ω)	Estimation error (%)	Estimated Value(F)	Estimation error (%)	Estimated Value(F)	Estimation error (%)
20	1.01e6	1	4.96e6	1	399e-12	0.2	10e-9	0
10	1.01e6	1	4.96e6	1	397e-12	1	10.0e-9	0
5	1.01e6	1	4.96e6	1	394e-12	2	10.0e-9	0

Table 6.13 The estimated values and estimation error of the coated metal model's parameters Vs. output's SNR (Rayleigh noise).

6.3 Discussion and Conclusion:

In this chapter, theAF based method used for EIS measurement is proposed. The accuracy of the AF-based method is tested for estimating the equivalent circuit's parameters representing Randles cell as well as the corroded coated metal models. The normalized estimation error is calculated for the two models in the case of noisy input and output data. A MATLAB program simulates the experiments and the following points are the main results of the test:

1. The AF –based method is adequate technique for impedance spectrum estimation in the case of noisy output. The maximum estimation error is2% for Randles Cell and 6% for coated metal at 5 dB SNR (Gaussian noise).
2. Compared with the HOS and FFT-based methods, the AF-based method estimates the impedance spectrum with same accuracy as the HOS and better than the FFT in the case of noisy output data with Gaussian distribution noise.
3. The AF –based method could not estimate the impedance spectrum properly in the case of noisy input. The minimum input's SNR at which the AF-based method is operational is 20 dBwhile it is 10 dBfor HOS-based method.

4. For electrolyte resistance (R1) estimation, the data measured at the whole frequency spectrum will be considered. For the rest of the parameters, the estimation is carried out at the low frequency band of the spectrum. However, the determination of the low frequency bandwidth is empirical.

CHAPTER 7

EIS DIFFERENT MEASUREMENTS COMPARISON (PRACTICAL EXPERIMENT):

In order to support the theoretical results obtained in chapters 5 and 6, an experiment is done using the instrument called Biologic VMP3 Multichannel workstation shown in Figure 7.1.[40]

Figure 7.1 Biologic VMP3 Multichannel workstation EIS system

The VMP3 is equipped with potentiostats and galvanostatic modes of operation which are capable of performing Electrochemical Impedance Spectroscopy (EIS) measurements. This option provides an integrated sine wave generator and frequency response analyzer features which are built onto the plug-in potentiostat module. The frequency range of the VMP3 is from 10 μHz to 1 MHzand it depends on the Fourier transform technique for measuring the impedance spectrum.

In the practical experiment, the VMP3 is used to measure the impedance spectrum of three systems:

1. Electrical circuit #1: represents a Randles Cell model with the parameters R1=10Ω, R2=100Ω and C1=100e-6F.(see Figure 7.2)
2. Electrical circuit #2: represents a coated metal model with the parameters R1=9.84KΩ, R2=9.77KΩ, R3=9.83KΩ, C1=8e-6F and C2=86e-6F.(refer toFigure 7.3)
3. Electrical circuit #3: The VMP3text Box -1 which is used for a calibration purposes. This box is an electrical circuit which can represents a coated metal. The parameters of the circuits are R1=5Ω, R2=1000Ω, R3=3570Ω, C1=10e-9F and C2=2.2e-6F.

Figure7.2: Randles cell circuit model.

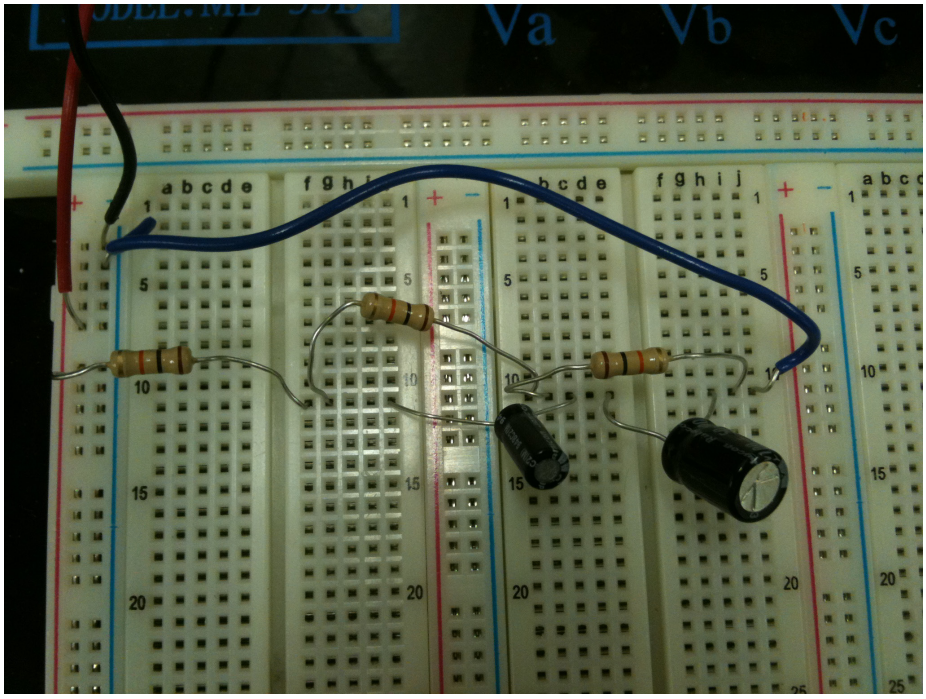

Figure7.3: Coated metal circuit model.

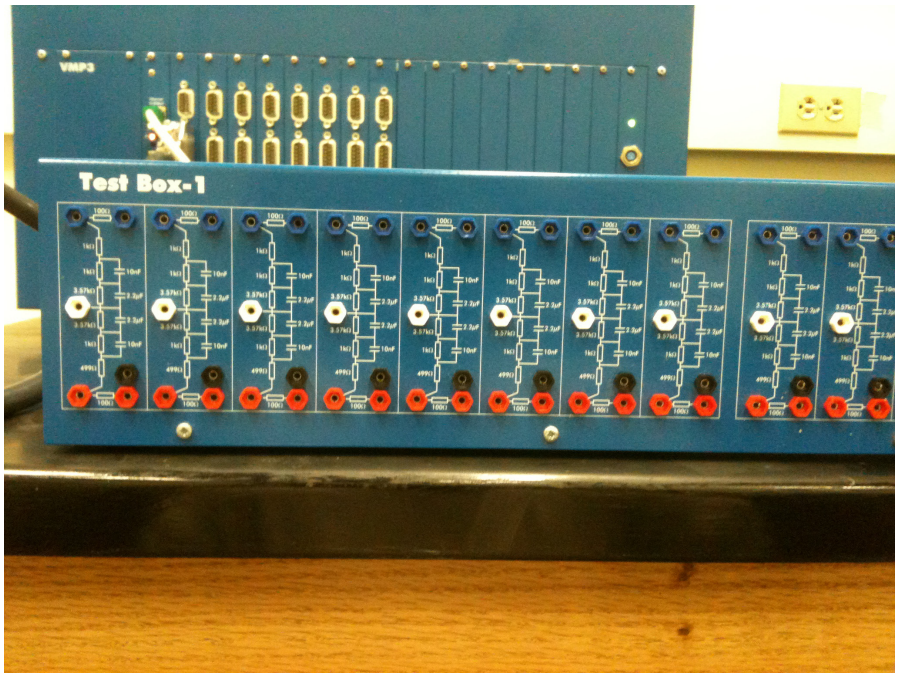

Figure 7.4: VMP3 Test Box-1.

7.1VMP3& HOS-based method Comparison:

In the experiment, the tested circuit is connected to one of the 16-independent VMP3 channels and software called EC-Lab measuresboth the impedance spectrum and parameters of the tested circuit. Figure 7.5 shows the setup of the experiment while Figure 7.6 displays a snapshot of the EC-Lab software.

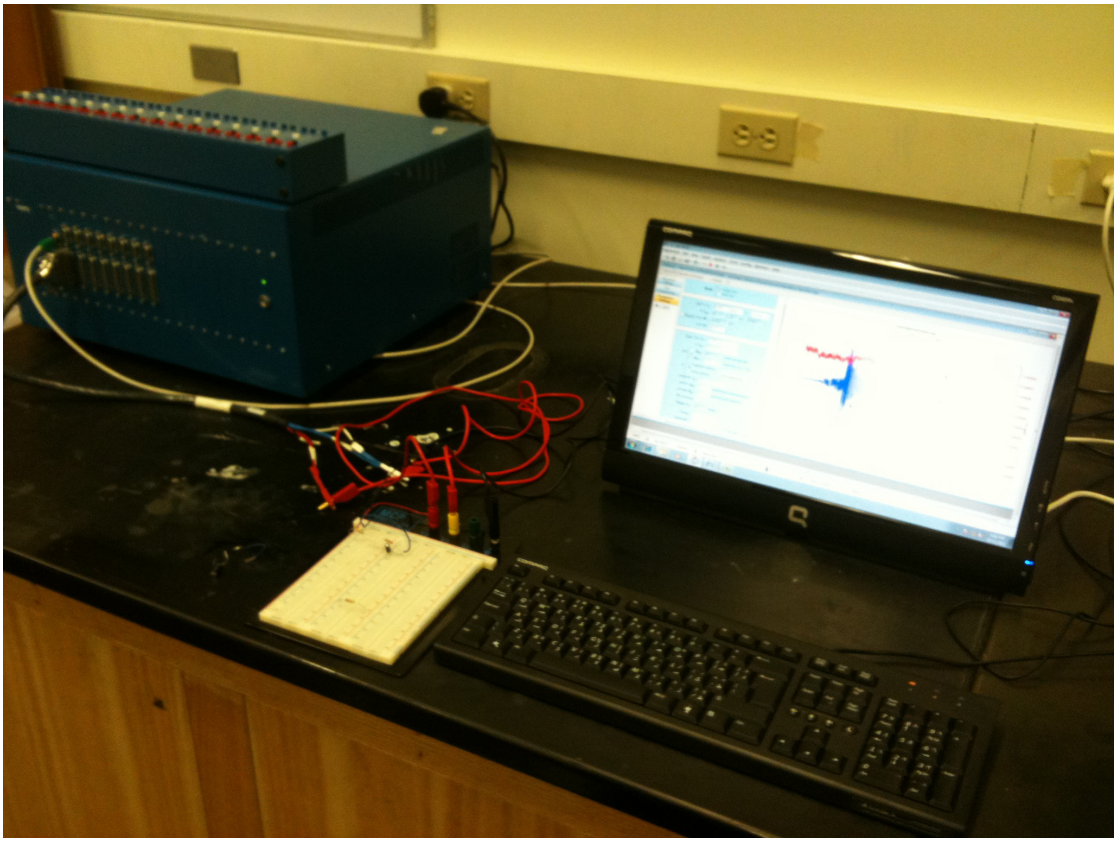

Figure 7.5: The Experiment Setup.

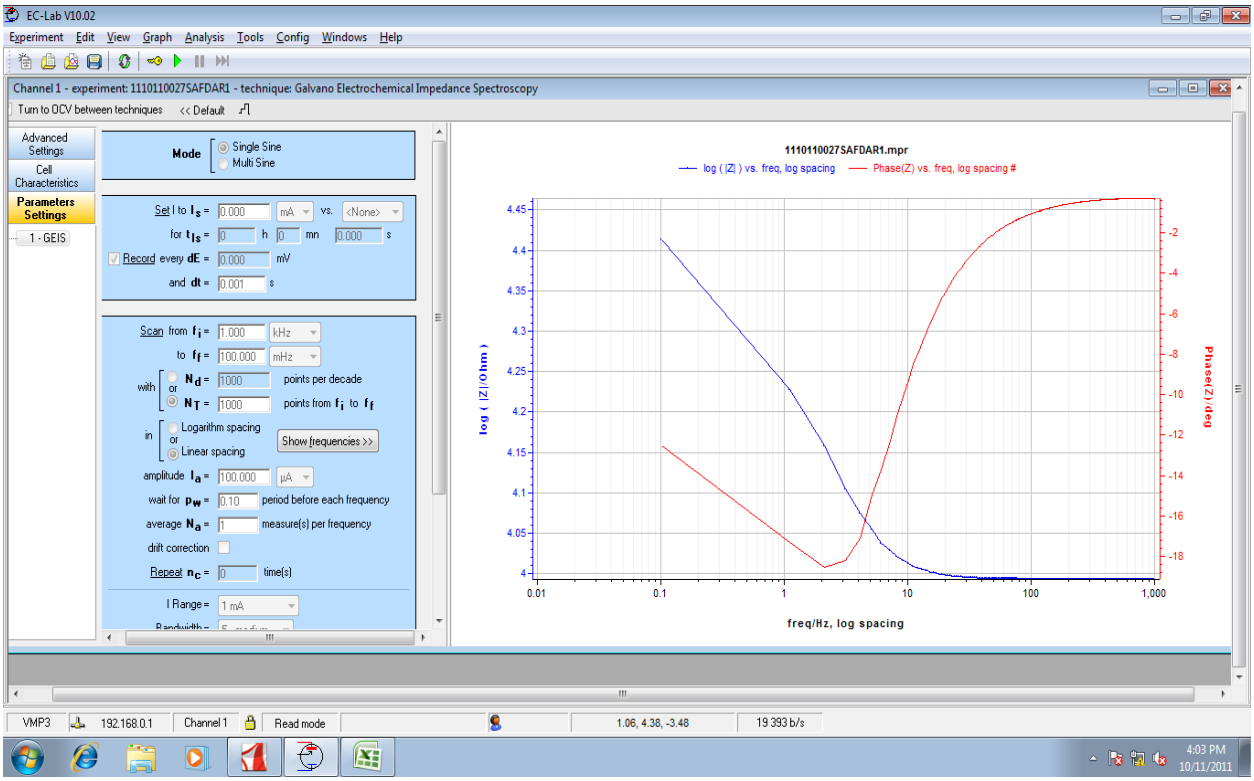

Figure 7.6: The EC-Lab configuration and result page.

For the Randles cell circuit model, it is observed that the VMP3 produces a very efficient estimation of the impedance spectrum with normalized estimation error of 0.01%.

In comparison with the HOS-based method, the same input and output signals produced by VMP3 obtained through the data acquisition property could not be used in the HOS-algorithm. This is because the obtained input signal is not sampled as per the Nyquist sampling rate. In addition, the 3rd order moment of the input signal is around zero which will make the HOS-based technique inactive. So, the comparison

is done between the experimental results of the VMP3 and the theoretical results (MATLAB simulation) of the HOS-based method. Based on the above comparison, the HOS-based method performs better than the VMP3 such that normalized impedance estimation error does not exceed 0.0006% while it is 0.01% in the case of VMP3. Figure 7.7a, b and c show the estimated impedance spectrum produced by both the HOS-based method and VMPS3 over two frequency sections (low and high).

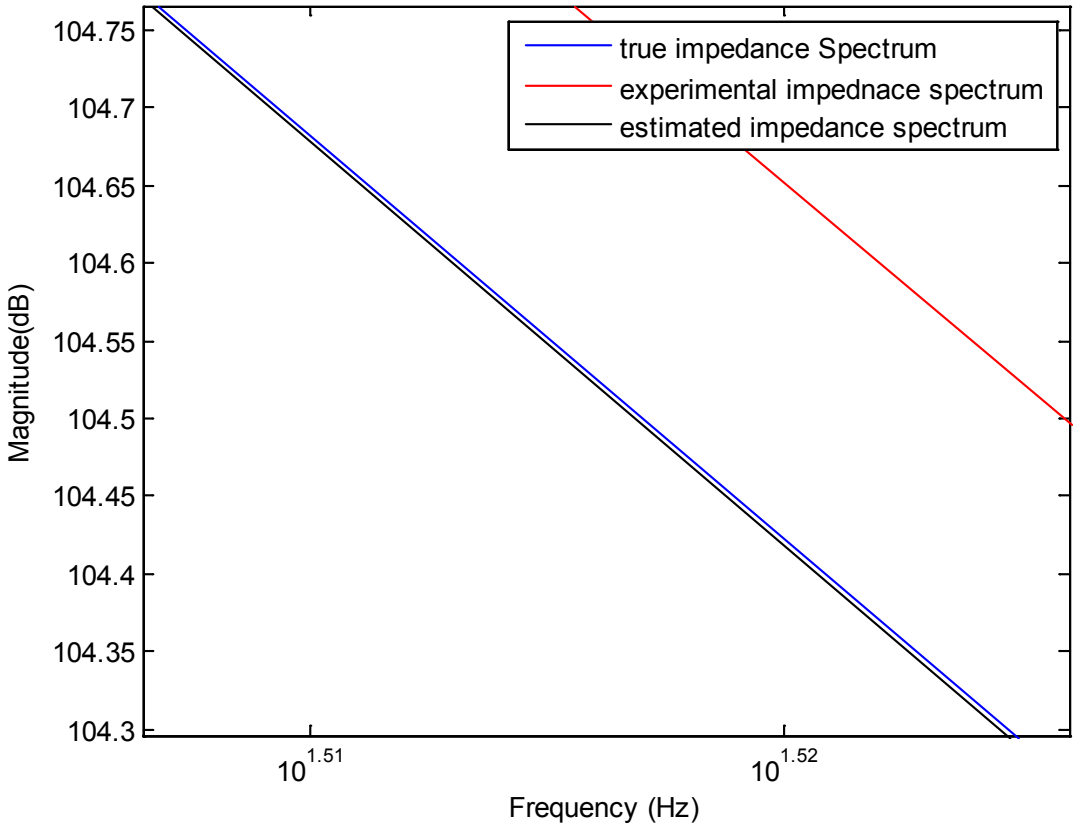

Figure 7.7a: The true amplitude impedance spectrum, experimental amplitude impedance spectrum (VMP3) and estimated amplitude impedance (HOS) spectrum over the low frequency side (Randles Cell model).

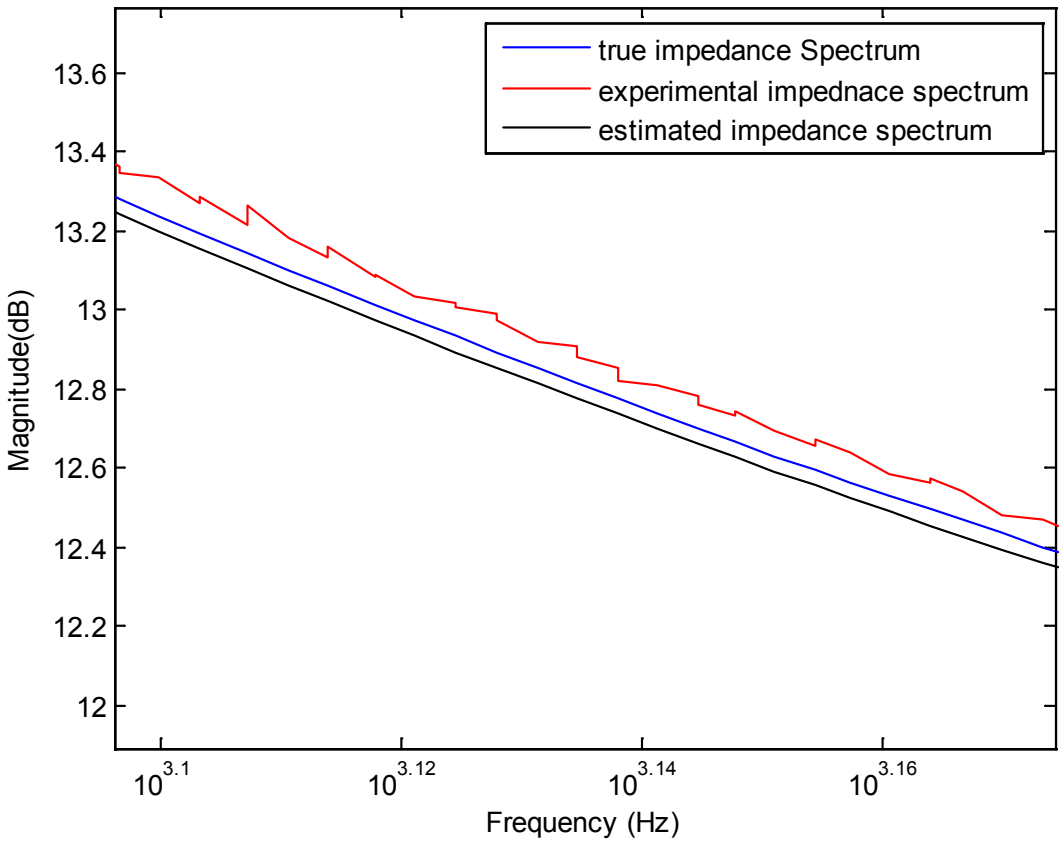

Figure 7.7b: The true amplitude impedance spectrum, experimental amplitude impedance spectrum (VMP3) and estimated amplitude impedance (HOS) spectrum over the high frequency side (Randles Cell model).

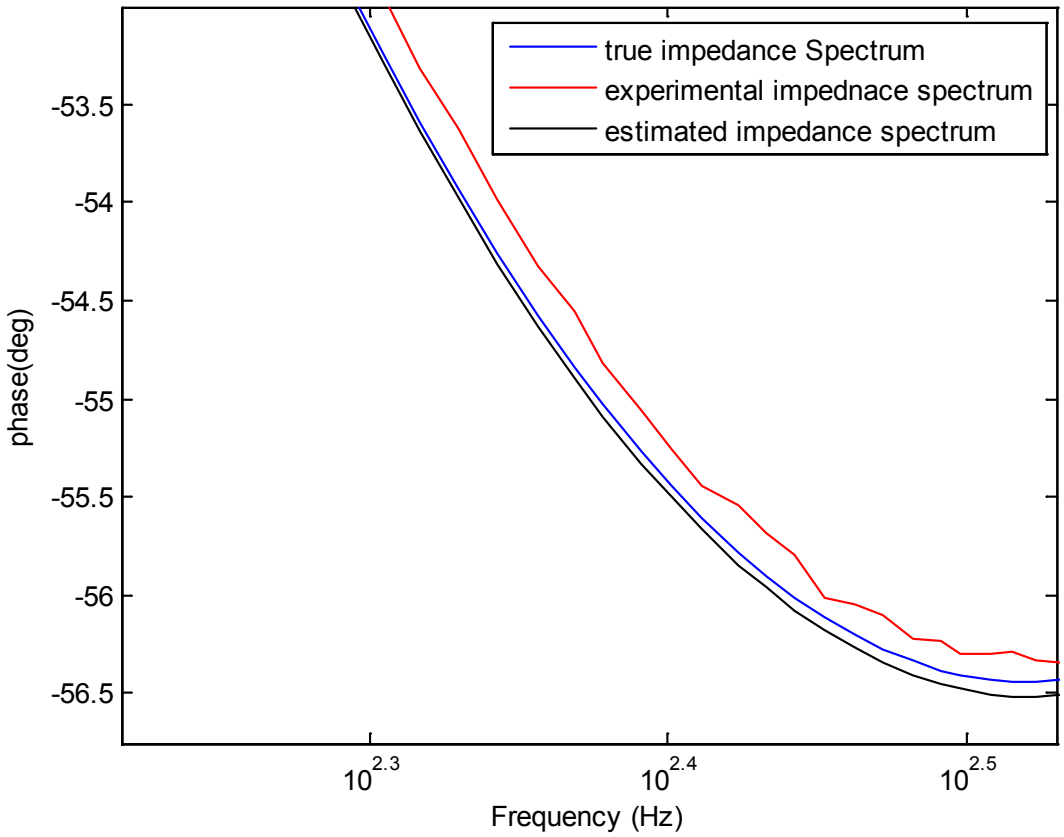

Figure 7.7c: The true phase impedance spectrum, experimental phase impedance spectrum (VMP3) and estimated phase impedance (HOS) spectrum (Randles Cell model).

Moreover, the HOS-based method shows efficient estimation even with the exist of the noise and its normalized estimation error at low output's SNR is close to the estimation error of VMP3 (see Table 7.1)

SNR(dB)	Normalized estimation error (%)
20	0.01
15	0.02
10	0.03
5	0.06

Table 7.1: Output's SNR (Gaussian) vs. the normalized estimation error of the estimated impedance spectrum for the Randles cell by the HOS-based method

Regarding the direct parameter estimation using AF techniques, it estimates the circuit parameters better than the VMP3 such that it gives the exact values of the parameters in the case of 20dB output's SNR (refer to Table 6.4).

The comparison ismade with other circuits that represent a coated metal. The coated metal can be represented with several models such as the two models shown in the Figure below [29]:

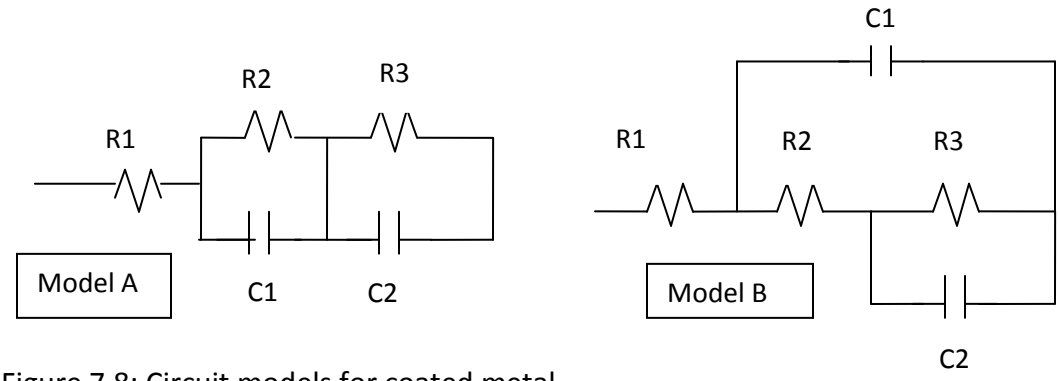

Figure 7.8: Circuit models for coated metal.

For both models, the experiment shows that he HOS –based method measures the impedance more precisely than the VMP3 in the frequency range : 1Hz-10kHz as shown in Figures 7.9 a, b (model A) and 7.9 c, d (model B):

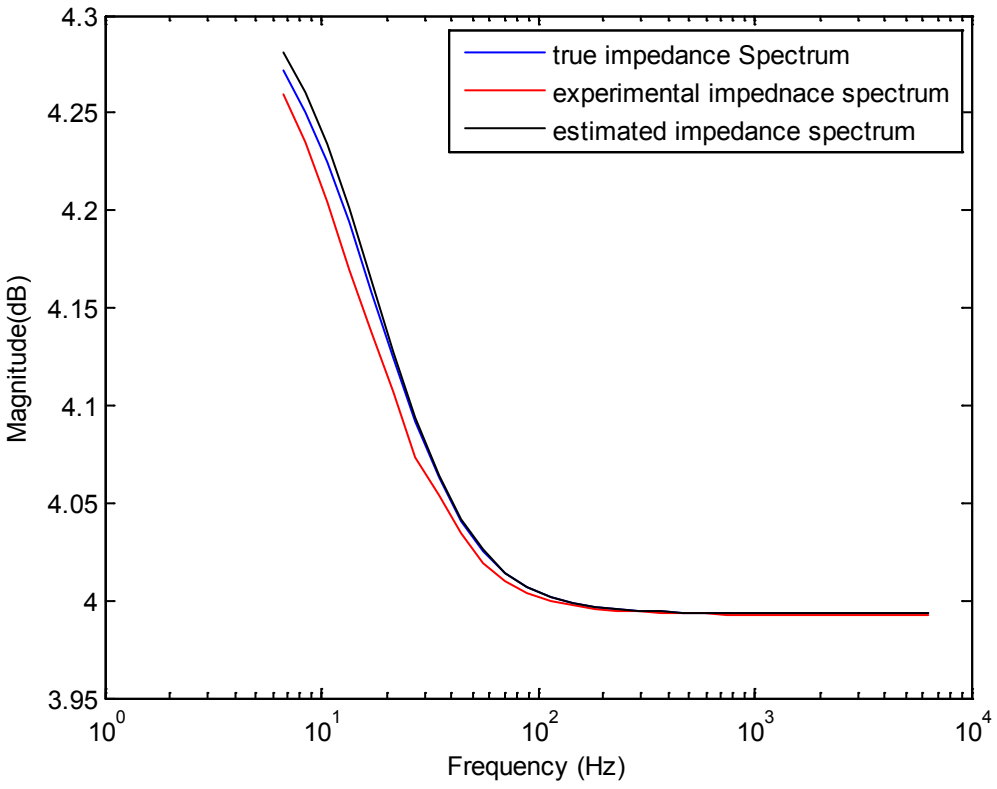

Figure 7.9a: The true amplitude impedance spectrum, experimental amplitude impedance spectrum (VMP3) and estimated amplitude impedance (HOS) for coated metal model A.

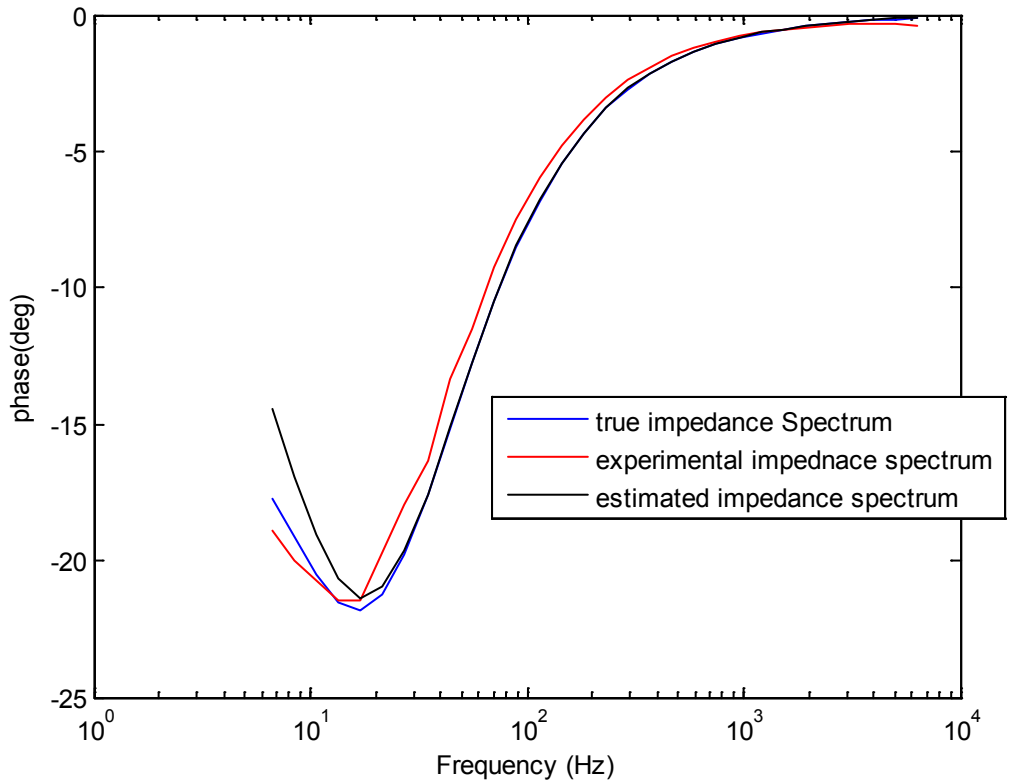

Figure 7.9b: The true phase impedance spectrum, experimental phase impedance spectrum (VMP3) and estimated phase impedance spectrum (HOS) for coated metal model A.

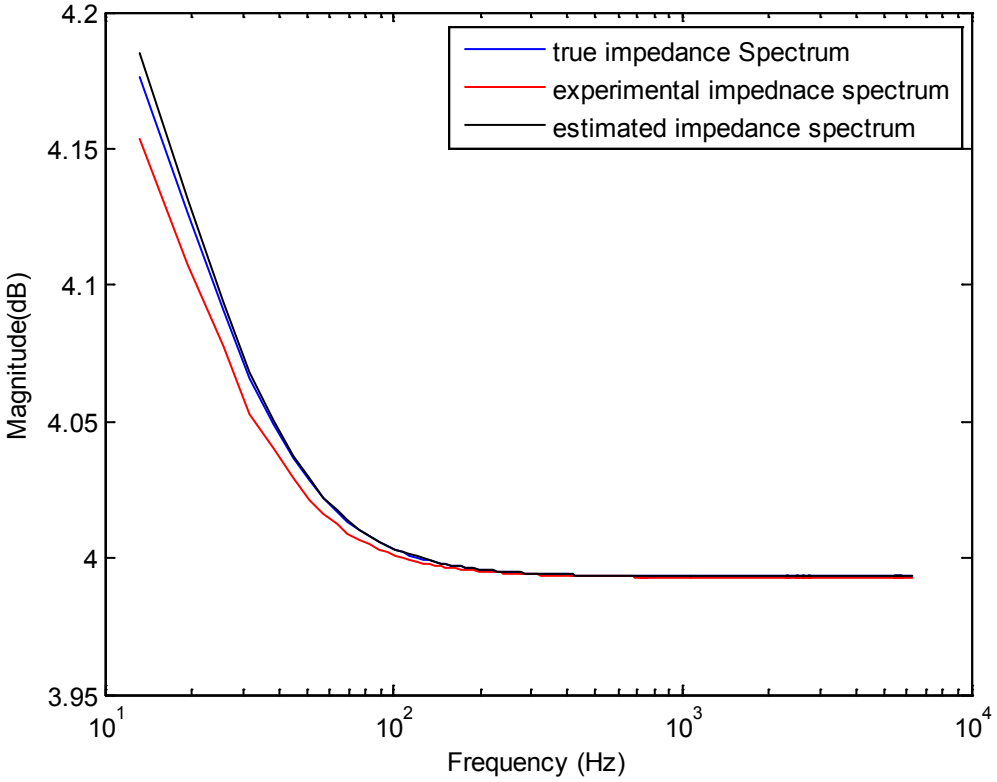

Figure 7.9c: The true amplitude impedance spectrum, experimental amplitude impedance spectrum (VMP3) and estimated amplitude impedance spectrum (HOS) for coated metal model B.

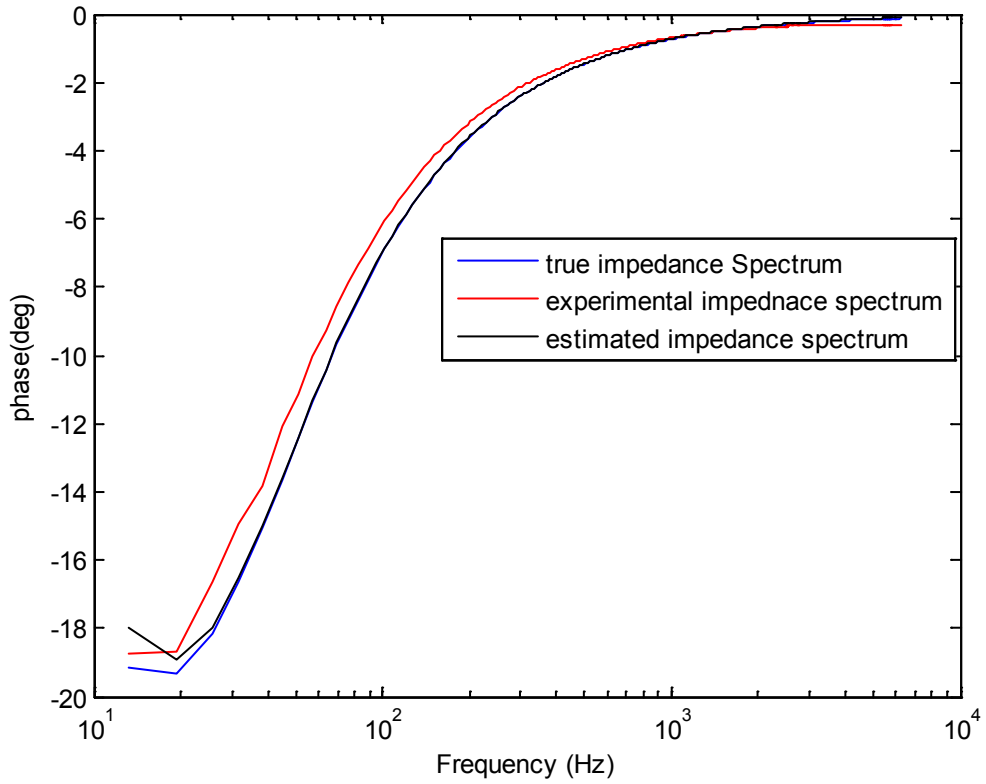

Figure 7.9d: The true phase impedance spectrum, experimental phase impedance spectrum (VMP3) and estimated phase impedance spectrum (HOS)for coated metal model B.

In addition, the normalized estimation error is reduced using the HOS-based method compared with VMP3 as per Table 7.2.

Circuit Model	Normalized Estimation Error HOS-based method	Normalized Estimation Error VMP3
A	0.06	0.1
B	0.0003	0.003

Table 7.2: Normalized estimation error for HOS-based method and VMP3 in estimating the circuit model A&B.

7.2VMP3 &AF-based method Comparison:

The test box-1 is used to compare the performance of the direct parameter estimation using AF-based method and the VMP3. The VMP3's input and output data could not be used as input to the AF algorithm since they are not uniformly spaced. So, the comparison is done between the experiment results of the VMP3 and the theoretical results (MATLAB simulation) of the AF-based method. The result illustrates that the AF-based method approximates the circuit parameters more accurately than the VMP3 as shown in Table 7.3.

Parameter	Estimator error (%) AF-based method	Estimator error (%) VMP3
R1	1.8	1
R2	0	1
R3	0.02	0.5
C1	5	12
C2	0	1

Table 7.3: Normalized estimation error for HOS-based method and VMP3 in estimating the circuit's parameters for Test Box-1.

7.3 Discussion and Conclusion:

In this chapter, the performance of the HOS and AF based methods is compared with experimental results produced by spectroscopy instrument called VMP3 (Bio-Logic).The results show that both the HOS and AF based methods execute the impedance measurements more accurate than the VMPS3 when a proper input signal is applied. For HOS-based method, the applied signal should be sampled as per the Nyquist theorem and the frequency band should be wide enough to cover the whole impedance spectrum. In addition, the 3^{rd} order cumulant of the applied signal should be greater than zero. For the AF based method, the input and output signals need to be uniformly sampled in the frequency domain.

CHAPTER 8

Conclusion

In conclusion, two new EIS measurements techniques are proposed in this thesis which are HOS deconvolution and AF based methods. These approaches are recommended to overcome the drawbacks of the existing EIS techniques in terms of noise immunity for time domain methods and long measurement timefor frequency domain methods. The HOS deconvolution based method depends on the third order moments of both the input and output signals which eliminates the symmetrical distribution noise signals. To reach the optimum performance of the HOS based technique, a proper selection of the applied signal is required to insure that the signal is non-Gaussian and has a wide frequency bandwidth. In addition, a suitable selection of the system's assumed order and the cumulant maximum lag parameter (M) are needed. Experimental and simulation results show the robustness of the HOS-based

method in the case of Gaussian and non-Gaussian noise distributions. The maximum normalized estimation error is 1% in the case of noisy output and 2% in the case of noisy input/output data. This maximum normalized estimation error is calculated at the worst scenario where the input and output signals are disturbed with non-Gaussian noise (Rayleigh) with input and output's SNR of 10dB and 5dB respectively.

The second proposed EIS method is applying adequate adaptive filtering (AF) algorithms in order to directly estimate the parameters of the equivalent circuit representing an electrochemical system. This is could be achieved by designing a cost function in terms of circuit parameters and choosing specific AF algorithm that performs optimistic minimization of the cost function. As per experimental and simulation results, the AF estimates the circuit's parameters precisely in the case of noisy output data.The maximum normalized estimation error is 2% for Randles Cell circuit and 6% for coated metal modelat 5 dB output'sSNR (Gaussian noise).

REFERENCES

[1] Byoung-Yong Chang and Su-Moon Park," Electrochemical Impedance Spectroscopy", Annual Review of Analytical Chemistry 2010.

[2]. Digby D. Macdonald," Reflections on the history of electrochemical impedance spectroscopy", ElectrochimicaActa 51 (2006) 1376–1388

[3] Digby D. Macdonald," A Brief History of Electrochemical Impedance Spectroscopy",Center for Electrochemical Science and Technology Pennsylvania State University.

[4] EvgenijBarsoukov J. Ross Macdonald," Impedance Spectroscopy Theory, Experiment, and Applications", Second Edition,2005.

[5]. J. ROSS Macdonald," Impedance Spectroscopy", Annals of Biomedical Engineering, Vol. 20, pp. 289-305, 1992

[6] Bernard A. Boukamp," Practical application of the Kramers-Kronig transformation on impedance measurements in solid state electrochemistry", Solid State Ionics 62 (1993) 131-141

[7] C.O. Yoon, E. Baroukov, J.H. Kim, Korea KumhoPetrochemical Co., Ltd., Us Patent 6687631, 2004.

[8] A. Lasia, Electrochemical Impedance Spectroscopy and Its Applications, Modern Aspects ofElectrochemistry, B. E. Conway, J. Bockris, and R.E. White, Edts., Kluwer Academic/PlenumPublishers, New York, 1999, Vol. 32, p. 143-248

[9] EvgenijBarsoukov , Sang HyoRyu, Hosull Lee" A novel impedance spectrometer based on carrier function Laplacetransformof the response to arbitrary excitation" JournalElectro analytical Chemistry 536 (2002) 109_/122

[10] ZHE-SHENG FENG, BAO-RUI SUN, JIA DING, ZI LIANG,"SPLINE INTERPOLATION UESED IN ELECTRONCHEMICAL IMPEDANCE SPECTROSCOPY",IEEE,2008

[11] Chao Yang, Daniel Rairigh, Andrew Mason "On-Chip Electrochemical Impedance Spectroscopy forBiosensor Arrays". IEEE SENSORS 2006, EXCO, Daegu, Korea

[12] J. L. Morrison1, W. H. Morrison,"Real Time Estimation of Battery Impedance", IEEEAC paper #1461,2006

[13] Mehdi Sadri, Abbas Shoulaie," A Practical Approach to Measure Battery's Internal Impedance", 1st Power Electronic & Drive Systems & Technologies Conference, IEEE 2010

[14] G. S. Popkirov and R. N. Schindler," A new impedance spectrometer for the investigation of electrochemical systems", Institute for Physical Chemistry,1992

[15] G. S. Popkirov and R. N. Schindler," Optimization of the perturbation signal for electrochemical impedance spectroscopy in the time domain", Institute for Physical Chemistry,1993

[16]. Xinjian Huang a, Huilian Chen a, Haiqiang Deng a, Lishi Wang a,⇑, Shijun Liao a, AiminTang "A fast andsimple electrochemical impedance spectroscopy measurement techniqueand its application in portable, low-cost instrument for impedimetricbiosensing", Journal of Electro analytical Chemistry 657 (2011) 158–163

[17].Jung-Suk Yoo and Su-Moon Park **"**An Electrochemical Impedance Measurement Technique Employing Fourier Transform" Anal. Chem. 2000, 72, 2035-2041.

[18].Jung-Suk Yoo, Inja Song, Ji-Hun Lee, and Su-Moon Park* Real-Time Impedance Measurements during Electrochemical Experiments and Their Application to Aniline Oxidation, Anal. Chem. 2003, 75, 3294-3300.

[19] Chao Yang, Daniel Rairigh, Andrew Mason," Fully Integrated Impedance SpectroscopySystems for Biochemical Sensor Array", IEEE,2007.

[20] J. Ross Macdonald "Precision of impedance spectroscopy estimates of bulk, reaction rate,and diffusion parameters,"J. Electroanal. Chem., 307 (1991) 1-11.

[21]Yamani, A., Bettayeb, M., "High Order Statistics-based deconvolutionof NDT Ultrasonic data,"SABIC Final Report(EE/SABIC/96-8),November 3,1998.

[22]G. B. Giannakis and J. M. Mendel," Identification of Nonminimum Phase Systems Using Higher Order Statistics", IEEE TRANSACTIONS ON ACOUSTICS. SPEECH. AND SIGNAL PROCESSING. VOL. 37, NO. 3. MARCH 1989.

[23] S.A. Alshebeili,∗ M.A. Alsehaili,∗ and M.A. Alkanhal"CUMULANTS AND GENETIC ALGORITHM FOR PARAMETERS ESTIMATION OF NONCAUSAL AUTOREGRESSIVE MODELS", International Journal of Modeling and Simulation, Vol. 22, No. 3, 2002

[24] John M. M. Anderson and Georgios B. Giannakis," Noisy InputlOutput System Identification Using Cumulants and the Steiglitz-McBride Algorithm ", IEEE TRANSACTIONS ON SIGNAL PROCESSING, VOL. 44, NO. 2, FEBRUARY 1996.

[25] K. STEIGLITZ AND L. E. MCBRIDE," A Technique for the Identification of Linear Systems", IEEE TR4NSACTIONS ON AUTOMATIC CONTROL, 1965

[26] John M. M. Anderson and William Edmonson," System Identification with Noisy Input–Output Data Using a Cumulant-Based Steiglitz–McBride Algorithm ", IEEE TRANSACTIONS ON CIRCUITS AND SYSTEMS—II: ANALOG AND DIGITAL SIGNAL PROCESSING, VOL. 44, NO. 5, MAY 1997.

[27] John M. M. Anderson and Georgios B. Giannala's," Noisy InputloutputSystemIdentification Using CumulantsandtheSteiglitz-McBride Algorithm",IEEE,1991

[28] **A.** Delopoulost and G. B. Giannakis," STRONGLY CONSISTENT OUTPUT ONLY AND INPUT/OUTPUT IDENTIFICATION IN THE PRESENCE OF GAUSSIAN NOISE",IEEE,1991

[29] Yamani, A., Bettayeb, M., UvaisQidwai," DEFECT DECONVOLUTION USING 3rdORDER STATISTICS FOR ULTRASONIC NONDESTRUCTIVE TESTING",IEEE,2007.

[30]M. CHETOUI 1, R.MALTI 1, M. THOMASSIN 3, M. AOUN 2, S. NAJAR 2, M.N. ABDELKRIM "THIRD-ORDER CUMULANTS BASED METHOD FOR CONTINUOUS-TIME ERRORS-IN-VARIABLES SYSTEM IDENTIFICATION BY FRACTIONAL MODELS", 2011 8th International Multi-Conference on Systems, Signals & Devices

[31] AnanthramSwami ,Jerry M. Mendel ,Chrysostomos L. (Max) Nikias "Higher-Order Spectral Analysis Toolbox User's Guide Version 2"

[32] Jerzy Hoja and GrzegorzLentka," Method Using Square-Pulse Excitation for High-Impedance Spectroscopy of Anticorrosion Coatings ", IEEE TRANSACTIONS ON INSTRUMENTATION AND MEASUREMENT, VOL. 60, NO. 3, MARCH 2011.

[33] J. R. Macdonald, LEVM Manual ver.7.11. CNLSImmittance Fitting Program. Farnborough, U.K.: Solartron Group Limited, 1999

[34] Henri Gavin "The Levenberg-Marquardt method for nonlinear least squares curve-fitting problems", Department of Civil and Environmental Engineering Duke University January 12, 2009

[35] Hiroomi Kunii*, YohsukeKinouchi," Parameter Estimation of Lumped Element Circuit for Tissue Impedance", Annual International Conference of the IEEE Enninee& in Medicine and Biolony Society, Vol. 20, No 6,1998

[36] Li Ran, Wu Junfeng, Wang haiying, Li Gechen," Prediction of State of Charge of Lithium-ionRechargeable Battery with Electrochemical Impedance Spectroscopy Theory ", 2010 5th IEEE Conference on Industrial Electronics and Applicationsis

[37] Aparna M. Dhirde, Nilesh V. Dale, HosseinSalehfar, Michael D. Mann, Tae-Hee Han," Equivalent Electric Circuit Modeling and Performance Analysis of a PEM Fuel CellStack Using Impedance Spectroscopy", IEEE TRANSACTIONS ON ENERGY CONVERSION, VOL. 25, NO. 3, SEPTEMBER 2010

[38] Bharath Pattipati1, Krishna Pattipati1, Jon P. Christopherson2,Setu Madhavi Namburu3,Danil V. Prokhorov3, and Liu Qiao3," Automotive Battery Management Systems", IEEE AUTOTESTCON 2008

[39] A. H. Sayed, Fundamentals of Adaptive Filtering, Wiley, NY, 2003.

[40] **EC**-Lab□ Software: Techniques and Applications Version 10.x – April 2010, Bi-Logic Science Instrument.

[41]Application Note "Basics of Electrochemical Impedance Spectroscopy", GamryInstrument,www.gamry.com

[42] Haiying Wang , GechenLi, ZhilongYu ,Xuefei Wang **"**Study on Genetic Algorithm in Estimating the Initial Value of EIS Equivalent Circuit" , IEEE 2009.

[43] Mathworks, "Control System Toolbox",http://www.mathworks.com/help/toolbox/control/

Nomenclature

AF	Adaptive Filtering
EIS	Electrochemical Impedance Spectroscopy
SD	Steepest Descent
LS	Least Square
HOS	High Order Statistics
SNR	Signal to Noise Ratio
NDT	Non Destructive Testing
FAR	Frequency Response Analyzer
PSD	Phase Sensitive Detection
FFT	Fat Fourier Transform
K-K	Kramers-Kronig
LTI	Linear Time Invariant
FIR	Finite Impulse Response
MPS	Minimum Phase System
NMPS	Non minimum Phase System
CNLS	Complex Nonlinear Least Square
i.i.d	Independent and identically distributed
$c_n^x(K_1, K_2, \dots K_{n-1})$	Nth order Cumulant of random process (x)
$m_n^x(K_1, K_2, \dots K_{n-1})$	Nth order moment of random process (x)
$m_n^G(K_1, K_2, \dots K_{n-1})$	Nth order moment of Gaussian random process (G)
$C_3^x(w_1, w_2)$	2nd order Spectrum (bi-spectrum) of random process (x)
$C_4^x(w_1, w_2, w_3)$	3rd order Spectrum (tri-spectrum) of random process (x)
n_a	Estimated dominator's order of H (Z), system frequency response
n_b	Estimated nominator's order of H (Z), system frequency response
$c^{vwv}(\tau_1, \tau_2)$	3rd order cross Cumulant between the input (v) and output (w)
$c^{vvv}(\tau_1, \tau_2)$	3rd order Auto Cumulant of the input signal (v)

VITA

Name	Saeed Omar Aljabri.
Religion	Islam.
Nationality	Saudi.
Place and Date of Birth	Yemen, 1980
Address	Alkohbar, Albayoniya 21th street Eastern Province, Saudi Arabia
E-mail Address	aljabrso@aramco.com aljabrso@hotmail.com
Contact information Mobile:	+966506822076

Education

Bachelor of Science in Electrical Engineering from King Fahd University of Petroleum and Minerals

Master of Science in Electrical Engineering from King Fahd University of Petroleum and Minerals